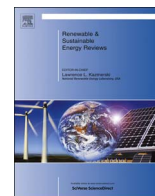




Contents lists available at ScienceDirect

## Renewable and Sustainable Energy Reviews

journal homepage: [www.elsevier.com/locate/rser](http://www.elsevier.com/locate/rser)

## Power electronics converters: Past, present and future

Guidong Zhang<sup>a,\*</sup>, Zhong Li<sup>b</sup>, Bo Zhang<sup>c</sup>, Wolfgang A. Halang<sup>b</sup><sup>a</sup> School of Automation, Guangdong University of Technology, Guangzhou, China<sup>b</sup> Faculty of Mathematics and Computer Science, Fernuniversität in Hagen, Germany<sup>c</sup> School of Electric Power, South China University of Technology, Guangzhou, China

## ARTICLE INFO

## Keywords:

Power electronics

Impedance-source

Power converters

Impedance-network matching

## ABSTRACT

The development of power electronics in the past century and the current state of the art of power electronics converters are briefly reviewed, before giving an insight into the deficiencies of the conventional current-source and voltage-source converters and into the superiority of impedance-source converters and, then, proposing a design methodology for impedance-source converters aimed to replace the traditional tedious, manual and experience-dependent design methods. Some examples for their deployment in renewable-energy applications are discussed, and the direction into which power electronic converters will develop in the future is indicated.

## 1. Introduction

In ancient times, thunder, lightning and electric fish [1] were the natural phenomena related to electricity. They were treated as myths, but not as energy until the discovery of electrostatic phenomena by Thales of Miletus in 640–540 BCE [2,3]. Much later in 1752, B. Franklin discovered electricity [4], and in 1820 H.C. Ørsted revealed electromagnetism [5]. Since then, a series of great discoveries on the principles of electricity and magnetism has been achieved by Volta, Coulomb, Gauß, Henry, Faraday and others, leading to many inventions such as batteries (1800), generators (1831), electric motors (1831), telegraphs (1837) and telephones (1876), to name just a few. In the early 19th century electricity has been established as a scientific discipline, and in the late 19th century the greatest progress has been witnessed in electrical engineering [6].

In 1882, the first power grid, which was a direct-current (DC) distribution system invented by T. Edison, was set up in New York to provide 110 V DC power supplying over 1000 bulbs in a short distance. At that time, the problem was how to transfer energy at a low loss from power plants to customers over a long distance through transmission lines [7]. It is now well known that electricity must be transmitted at high voltages and in the form of alternating current (AC), because DC voltage could not be increased or decreased by DC systems at that time [8]. In 1885, L. Gaulard and J.D. Gibbs developed a device named transformer, which can increase or decrease the electrical voltage of AC systems. Thereafter, G. Westinghouse applied transformers in AC distribution systems to transmit electricity efficiently over long distances, which has promoted the development of electrical engineering [5].

Transformers played a vital rôle in electricity transmission, especially in energy conversion between different voltages. Transformers can, however, only increase or decrease AC voltage (AC-AC) at the same frequency. Moreover, energy loss in transformers, magnetic radiations, huge volume and high cost of copper limited their wider use [9]. In practical applications, electric energy was expected to be converted from one form to another, for instance, between AC and DC, or just to different voltages or frequencies, or some combinations of those — demands that cannot be fully met by transformers. Therefore, novel techniques were required to solve those problems. With the development of semiconductor switches, power electronics has come into being [10].

Power electronics refers to electric power, electronics and control systems. Electric power deals with static and rotating power equipment for generation, transmission and distribution of electric power; while electronics is concerned with solid-state semiconductor power devices and circuits together with control systems for power conversion specified to meet the desired control objectives. Power electronics is one of the main technologies to realise energy conversion with high efficiency. It is known that about 70% of electric energy is converted by power electronics devices before it reaches the consumer. Nowadays, power electronics has become a fundamental technology critical for the development of energy conservation, especially for renewable energy [11].

The history of power electronics is linked to the breakthrough and the evolution of power-semiconductor devices. The first power electronics device was the mercury arc rectifier developed in 1900, followed by other power devices, like metal-tank rectifier, grid-controlled vacuum tube rectifier, ignitron, phanotron, thyatron and magnetic amplifier,

\* Corresponding author.

E-mail address: [zgdscut@gmail.com](mailto:zgdscut@gmail.com) (G. Zhang).<http://dx.doi.org/10.1016/j.rser.2017.05.290>Received 24 May 2016; Received in revised form 21 April 2017; Accepted 29 May 2017  
1364-0321/ © 2017 Elsevier Ltd. All rights reserved.

developed and deployed gradually for power-control applications until the 1950s. The second electronics revolution began in 1958 with the development of the commercial-grade thyristor by the General Electric company (GE), indicating the beginning of a new era of power electronics. From 1975 to 1995, more turn-off power-semiconductor elements have been developed and implemented, which have vastly improved modern electronics. Included here are improved bipolar transistors (with fine structures, and also shorter switching times), metal-oxide-semiconductor field-effect transistors (MOSFETs), gate turn-off thyristors (GTOs) and insulated-gate bipolar transistors (IGBTs). Correspondingly, many different types of power-semiconductor devices and power-conversion techniques have been proposed and designed. The power electronics revolution has endowed us with the ability to convert, shape and control electrical power [10].

With the development of semiconductor devices, different kinds of control strategies have also been developed to realise specified purposes. For instance, high-accuracy and high-frequency control methods based on single-chip solutions like Digital Signal Processors, Field Programmable Gate Arrays or Complex Programmable Logic Devices are applied to meet desired requirements and to gain better control of loads; more accurate mathematical methods to model power converters enable gaining better output features, reducing energy losses and increasing efficiency; and improved control algorithms are utilised to improve efficiency and robustness, to reduce complexity and to achieve better output features.

Power electronics converters fall into four categories, i.e. AC-DC, AC-AC, DC-DC and DC-AC converters, and they have been invented for and found a wide spectrum of applications in, for instance, transportation (electric/hybrid electric vehicles, electric locomotives, electric trucks), utilities (line transformers, generating systems, grid interfaces for alternative energy resources like solar panels, wind turbines and fuel cells, energy storage), industry/commerce (motor drive systems, electric machinery and tools, process control, factory automation), consumer products (air conditioners/heat pumps, appliances, computers, lighting, telecommunication equipment, un-interruptible power supplies, battery chargers) or medicine. Especially in the area of renewable energy applications, power electronics converters play a more important rôle, which enable DC micro-grids to realise high-efficient usage of renewable energy, and stable interfaces between energy storage systems and renewable energy resources [12,13], as well electrification of distant villages and rural areas [14]; high-voltage direct current (HVDC) systems can be also enabled to replace some long-range transmission AC transmission systems [15]; aircraft power supplies with special requirements can be realised by specific power converters [16]; to list just a few. Thus, power electronics has established itself as a scientific discipline [17].

With the rapid development of modern industry, power electronics is facing severe problems, namely how to meet the requirements of the load; how to improve the efficiency and reliability of power-semiconductor devices; how to design converters with smaller volume, less weight and lower cost; how to reduce the number of power switches and, thus, the design complexity of converters and how to improve the robustness of entire systems; and how to minimise negative influences on other equipment in electric power systems and on the electromagnetic environment [18].

Facing these challenges, some advances have been witnessed with respect to semiconductor switches of power converters, for example, integrated gate-commutated thyristors (IGCT) were invented to have lower conduction loss compared to the traditional high-capacity switches. Accordingly, control strategies were also improved [19].

To design a new power electronics converter, one can, on one hand, develop a new control strategy; on the other hand, one can design a novel power converter topology, so as to achieve specific outputs, simpler control, higher efficiency, less complexity, lower weight, minimal cost and better robustness. In fact, a control strategy is specified for a certain topology, and the topology determines the

control system. Therefore, it is of great significance to coin optimal power-converter topologies to fulfill the requirements of various applications.

Owing to a converter's input source being either a voltage source or a current source, various traditional converters fall into two categories: voltage-source and current-source converters. It is, however, known that voltage-source converters suffer from shoot-through problems, the applicability to capacitive loads only, and limited output-voltage gains; while current-source converters have open-circuit problems, are applicable to inductive loads only, and have limited output-current gains [20].

In order to solve these problems, the Z-source converter was first proposed by Peng in 2002 [21], coupling an LC impedance-network (a two-port network with a combination of two basic linear energy-storage elements, i.e. L and C) with a DC source to form a novel source, named Z-source, which is a kind of impedance-source (Z stands for impedance) [22,23,27,24–26]. An impedance-source can be regarded as a general source, including the current and the voltage sources as two extreme cases, i.e. an impedance-source can be regarded as a current source when its equivalent impedance tends towards infinity, and as a voltage source when its equivalent impedance is equal to zero. The concept of the impedance-source provides a solution to the problems existing in the traction converters and facilitates high efficiency of energy conversion [28–31].

Since 2002, many novel impedance-source converters with various topologies have been coined, such as quasi-Z-source converters, trans-Z-source converters, embedded-Z-source converters, which have been widely applied in wind energy [32], solar cells [33,34], motor drives [35,36], and vehicle systems [37–39]. However, the design of an impedance-source converter is still an art, lacking systematic design methodology, which hinders the extensive application of impedance-source converters in practice.

It is remarked that designing an impedance-source converter should be subject to the impedance-network matching, which instructs how an impedance-network can be matched to the sources, leading to a systematic design methodology, which will be discussed in detail in this paper.

The main part of this paper is organised as follows.

*Past of power electronics converters:* Section 1 expounds the history of the development of power electronics and power converters and, Section 2 gives preliminaries of traditional voltage- and current-source converters as well as Z-source converters.

*Present of power electronics converters:* A profound analysis of voltage- and current-source inverters is carried out in Section 3, and that of Z-source inverters in Section 4. The state-of-the-art of impedance-source converters together with typical examples are given in Section 5.

*Future of power electronics converters:* The impedance-network matching is clarified in Section 6, based on which a design methodology is proposed in Section 7. Some case studies for different industrial applications are presented in Section 8. Finally, Section 9 draws a conclusion and points out the direction that impedance-source converters should follow in the future.

## 2. Preliminaries

### 2.1. Voltage sources and current sources

A power converter processes an energy flow between two sources, i.e. generally between a generator and a load, as illustrated in Fig. 1. An ideal static converter is assumed to transmit electric energy between the two sources with 100% efficiency. The conversion efficiency is the main concern in designing a converter. In practice, power converter design therefore aims to improve efficiency.

There are two types of sources, namely voltage and current sources, any of which could be either a generator or a load.

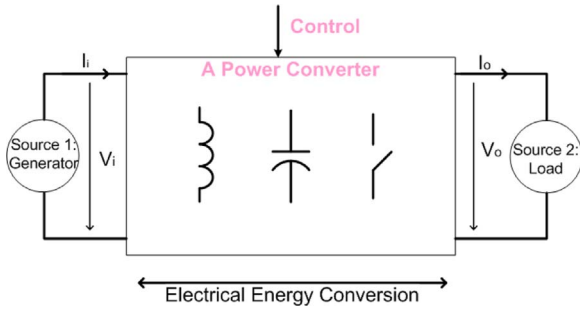


Fig. 1. A power converter.

A real voltage source can be represented as an ideal voltage source in series with a resistance  $r_{VS}$ , with the ideal voltage source having zero resistance, to ensure its output voltage to be constant. The voltage source is normally equivalent to a capacitor  $C$  with infinite capacitance, i.e.  $C = \infty$ , so that  $r_C = Z_C = -j\frac{1}{\omega C} \approx 0$ , where  $Z_C$  denotes the resistance of the capacitor.

Similarly, a real current source can be represented as an ideal current source in parallel with a resistance  $r_{CS}$ , with the ideal current source having infinite resistance, so that its output current is constant, which is normally equivalent to an inductor with infinite inductance, i.e.  $L = \infty$ , which implies also  $r_L = Z_L = j\omega L \approx \infty$ , where  $Z_L$  represents the resistance of the inductor.

Correspondingly, converters can be classified into voltage-source converters and current-source converters.

## 2.2. Impedance-network and Z-source

### 2.2.1. Impedance

The term ‘resistance’ is just concerned with DC circuits, which is extended to ‘impedance’ in case of applying to both DC and AC circuits. Therefore, for DC circuits, resistance and impedance are equivalent. Unlike resistance, which has only magnitude and is represented as a *positive* real number (of the dimension Ohm ( $\Omega$ )), impedance possesses both magnitude and phase, and can be represented as a complex number with the imaginary part denoting reactance and the real part representing resistance.

Impedance is used to measure the opposition that a circuit presents to a current when a voltage is applied [40], and is defined as the frequency-domain ration of the voltage to the current. For a sinusoidal current or voltage input, the polar form of the complex impedance relates amplitude and phase of the voltage or current. In particular,

- the magnitude of the complex impedance is the ratio of the voltage amplitude to the current amplitude, and
- the phase of the complex impedance is the phase shift by which the current lags or leads the voltage.

### 2.2.2. Impedance-network and two-port network

Like a resistor network, which is a collection of interconnected resistors in series or/and parallel, in the context of power electronics an impedance-network, which involves nonlinear switches, is a network of impedance components like switches, sources, inductors and capacitors, interconnected in series or/and parallel. An impedance-network can be passive, if it is just composed of inductors and/or capacitors, or active, if it is constituted of switches and/or diodes, inductors and/or capacitors.

It is difficult, if not impossible, to analyse an impedance-network using (linear) circuit theory due to the nonlinear switching components contained. It is, however, helpful to simplify the analysis of an impedance-network by reducing the number of its components, which is normally done by replacing the actual components with notional components of the same functions. Among existing analysis methods,



Fig. 2. Two-port network.

such as nodal and mesh methods [41], the concept of two-port networks is well suited to analyse impedance-networks [42].

A two-port network, as shown in Fig. 2, is an electrical network or a device with four terminals, which are arranged into two pairs called ports, i.e. each pair of terminals is one port. As shown in Fig. 2, the left port is usually regarded as the input port, while the right one is the output port. Therefore, a two-port network is represented by four external variables, i.e. voltage  $U_1(s)$  and current  $I_1(s)$  at the input port, and voltage  $U_2(s)$  and current  $I_2(s)$  at the output port, so that the two-port network can be treated as a black box modeled by the relationships between the four variables  $U_1(s)$ ,  $I_1(s)$ ,  $U_2(s)$  and  $I_2(s)$  [43,44].

The transmission equation of a two-port network is given by [45]:

$$\begin{bmatrix} U_1(s) \\ I_1(s) \end{bmatrix} = \mathbf{A}(s) \cdot \begin{bmatrix} U_2(s) \\ -I_2(s) \end{bmatrix}, \quad (1)$$

where  $\mathbf{A}(s)$  is the transmission matrix and written as

$$\mathbf{A}(s) = \begin{bmatrix} A_{11}(s) & A_{12}(s) \\ A_{21}(s) & A_{22}(s) \end{bmatrix}, \quad (2)$$

whose elements are defined as

$$\begin{cases} A_{11}(s) = \left. \frac{U_1(s)}{U_2(s)} \right|_{I_2(s)=0}, \\ A_{12}(s) = \left. \frac{U_1(s)}{-I_2(s)} \right|_{U_2(s)=0}, \\ A_{21}(s) = \left. \frac{I_1(s)}{U_2} \right|_{I_2(s)=0}, \\ A_{22}(s) = \left. \frac{I_1(s)}{-I_2(s)} \right|_{U_2(s)=0}. \end{cases} \quad (3)$$

Therefore, (1) can be rewritten as

$$\begin{cases} U_1(s) = A_{11}(s)U_2(s) + A_{12}(s)(-I_2(s)), \\ I_1(s) = A_{21}(s)U_2(s) + A_{22}(s)(-I_2(s)). \end{cases} \quad (4)$$

A two-port network model is a mathematical circuit-analysis technique allowing to represent a complex circuit by a simple notation. A two-port network is regarded as a black box with its properties specified by a matrix of numbers, which allows to easily calculate the network's response to signals applied to the ports, without solving for all the internal voltages and currents in the network [46].

Impedance-networks can have multiple ports connecting external circuits, but generally they have two ports, and can thus be equivalent to a two-port network. In terms of Thevenin's equivalent impedance theorem, the *input impedance* of a two-port network is the equivalent impedance of the two-port network with an open input port and an output port connecting a load; while the *output impedance* (also named *source impedance* or *internal impedance*) is the equivalent impedance of the two-port network with a short-circuited input port and an open output port. Further in terms of Ohm's law, the input impedance of a two-port network  $Z_i(s)$  reads

$$Z_i(s) = \frac{U_1(s)}{I_1(s)} = \frac{A_{11}(s)Z_L(s) + A_{12}(s)}{A_{21}(s)Z_L(s) + A_{22}(s)}, \quad (5)$$

where  $Z_L(s)$  is the load impedance of the two-port network's output

port. Similarly, the output impedance of a two-port network  $Z_o(s)$  reads

$$Z_o(s) = \frac{U_2(s)}{I_2(s)} = \frac{A_{22}(s)Z_S(s) + A_{12}(s)}{A_{21}(s)Z_S(s) + A_{11}(s)}, \quad (6)$$

where  $Z_S(s)$  is the source impedance of the two-port network's input port.

### 2.2.3. Impedance-source converters (Z-source converters)

An impedance-network together with a source constitutes an *impedance-source* (also named Z-source), with its equivalent impedance  $Z \in [0, +\infty)$ . The impedance-source is a general source in the sense that it includes voltage and current sources as its extreme cases, that is, it becomes a voltage source for  $Z = 0$ , and a current source for  $Z \rightarrow \infty$ . It can then exhibit rich properties for  $0 \leq Z < \infty$ .

Correspondingly, an impedance-source converter is coined, which possesses unique advantages over traditional voltage- and current-source converters, and can well meet more stringent industrial requirements. It is known that voltage-source converters suffer from shoot-through problems, the inapplicability to a capacitive load, and limited gains of output voltages; while current-source converters have open-circuit problems, are inapplicable to an inductive load, and have limited gains of output currents. A well designed impedance-source converter can overcome these problems.

## 3. Voltage-source and current-source inverters

Converter is a general term for AC-DC rectifiers, DC-DC choppers, DC-AC inverters and AC-AC converters. AC-DC rectifiers and AC-AC converters may have the problems of shoot-through, open-circuit and limited output gains, while DC-DC choppers may suffer from the shoot-through and open-circuit problems and the inapplicability to a capacitive or inductive load, and DC-AC inverters may even have all of the problems mentioned. For simplicity, voltage-source and current-source inverters are taken as examples to be qualitatively analysed from the perspective of impedance-networks.

Voltage-source and current-source inverters are depicted in Fig. 3, where  $V_{VS}(s)$  and  $I_{VS}(s)$  in Fig. 3(a) represent voltage and current of the voltage source; while  $V_{CS}(s)$  and  $I_{CS}(s)$  in Fig. 3(b) stand for voltage and current of the current source, respectively. Furthermore, their equivalent circuits are drawn in Fig. 4, where  $Z_{VS}(s)$  and  $Z_L(s)$  are the equivalent source impedance and equivalent load impedance of the voltage-source inverter in Fig. 4(a), whose corresponding two-port network is indicated in the dashed box in Fig. 4(a), and where  $Z_{VS}(s)$  is the unique component in the two-port network, while  $Y_{CS}(s)$  and  $Y_L(s)$  are the equivalent source admittance and load admittance of the current-source inverter in Fig. 4(b), whose corresponding two-port network is shown in the dashed box in Fig. 4(b), where  $Y_{CS}(s)$  is also the unique component in the two-port network.

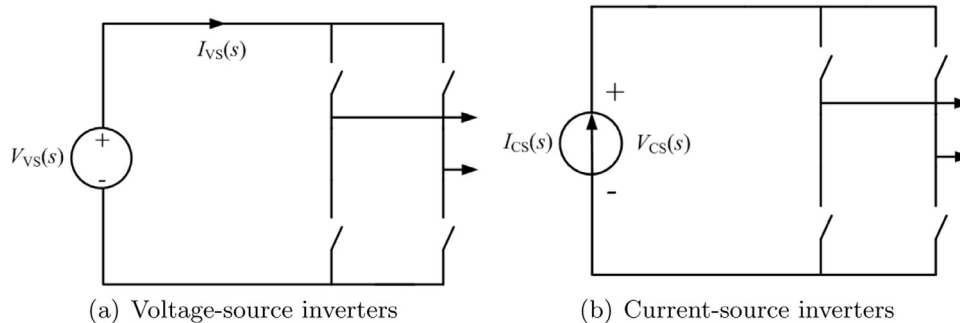


Fig. 3. Voltage-source and current-source inverters.

### 3.1. Voltage-source inverters

#### 3.1.1. Shoot-through

In terms of (3), the transmission matrix of the voltage-source inverter in Fig. 4(a) reads

$$\begin{cases} A_{V11}(s) = 1, \\ A_{V12}(s) = Z_{VS}(s), \\ A_{V21}(s) = 0, \\ A_{V22}(s) = 1. \end{cases} \quad (7)$$

Substituting (7) into (5) results in the input impedance of the voltage-source inverter as

$$Z_i(s) = \frac{A_{V11}(s)Z_L(s) + A_{V12}(s)}{A_{V21}(s)Z_L(s) + A_{V22}(s)} = Z_L(s) + Z_{VS}(s), \quad (8)$$

while the input current of the voltage source is thus obtained as

$$I_{VS}(s) = \frac{V_{VS}(s)}{Z_i(s)} = \frac{V_{VS}(s)}{Z_L(s) + Z_{VS}(s)}. \quad (9)$$

It is obvious that  $Z_L(s) = 0$  in case the switches of the voltage-source inverter on a bridge are turned on simultaneously. Moreover, the source impedance  $Z_{VS}(s)$  is normally very small, i.e.  $Z_{VS}(s) \approx 0$ . Therefore,  $Z_i(s) = Z_L(s) + Z_{VS}(s) \approx 0$ , which implies  $I_{VS}(s) \rightarrow \infty$ . Thus, the voltage source is shorted and a very large current will destroy the switches. This is the so-called *shoot-through problem*.

In order to prevent shoot-throughs to occur, the dead-time compensation technique has often been adopted to prevent switches from turning on simultaneously [47].

#### 3.1.2. Limited output-voltage gain

In terms of Fig. 4(a), substituting  $Z_S(s) = 0$  and (7) into (6) results in the inverter's output impedance as

$$Z_o(s) = \frac{A_{V22}(s)Z_S(s) + A_{V12}(s)}{A_{V21}(s)Z_S(s) + A_{V11}(s)} = Z_{VS}(s). \quad (10)$$

Obviously, the voltage of the load can be expressed as

$$V_{VL}(s) = V_{VS}(s) - I_L(s)Z_{VS}(s). \quad (11)$$

It is straightforward from (11) that  $Z_{VL}(s) \leq V_{VS}(s)$  due to  $Z_{VS}(s) \geq 0$  and  $I_L(s) \geq 0$ , i.e. the load voltage  $V_{VL}(s)$  is lower than or equal to the source voltage  $V_{VS}(s)$ .

In order to fulfill the requirements for high output-voltage gain of industrial applications such as solar power generation, DC-DC boost front-stage converters can be cascaded to boost the output voltage, which has actually changed their output-impedance features [48].

#### 3.1.3. Inapplicability to capacitive loads

It is known that electrical loads can be classified into resistive, capacitive and inductive ones. A capacitive load is an AC electrical load, in which the current reaches its peak before the voltage, while an inductive load is a load that pulls a large amount of current when first

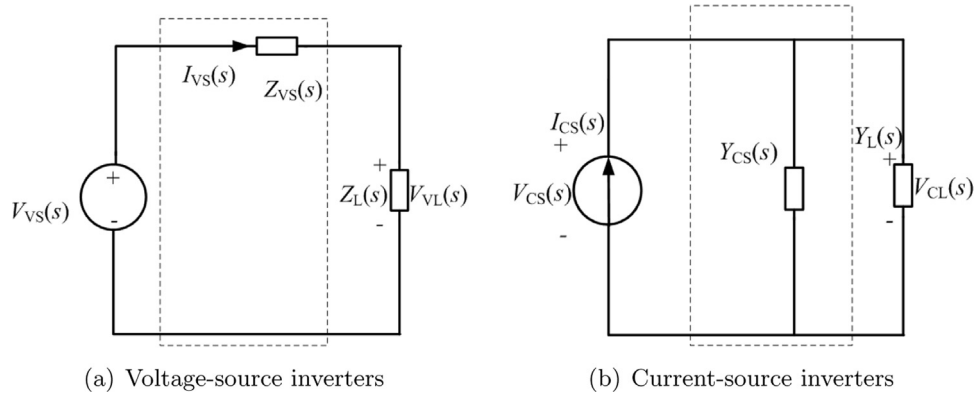


Fig. 4. Equivalent circuits of voltage-source and current-source inverters with two-port networks.

energised, as in motors, transformers and wound control gear, and a resistive load is a load which consumes electrical energy in a sinusoidal manner. This means that the current flow is in time with and directly proportional to the voltage, such as with incandescent lighting and electrical heaters.

The impedance  $Z_{Vs}(s)$  in a two-port network is equivalent to a capacitor with very large capacitance, which implies that  $Z_{Vs}(s) = -j\frac{1}{\omega C} \approx 0$ . In terms of (11), one has  $V_{VL}(s) = V_{Vs}(s)$ . It is remarked that if the load impedance  $Z_L(s)$  is capacitive, a capacitive source offers energy to a capacitive load, while  $V_{VL}(s) = V_{Vs}(s)$  at a steady state implies that the voltage-source inverter does not function, and is thus inapplicable to capacitive loads.

It is concluded that, due to the impedance of a two-port network between the voltage source and the inverter bridges, the voltage-source inverter has the problems of shoot-through, limited output-voltage gains and inapplicability to capacitive loads, which restrain its wide utilisation.

### 3.2. Current-source inverters

#### 3.2.1. Open circuit

In terms of (3), the transmission matrix of the current-source inverter in Fig. 4(b) reads

$$\begin{cases} A_{C11}(s) = 1, \\ A_{C12}(s) = 0, \\ A_{C21}(s) = Y_{Cs}(s), \\ A_{C22}(s) = 1, \end{cases} \quad (12)$$

where  $Y_{Cs}(s)$  is the source admittance of the current-source inverter, which is reciprocal to its source impedance. Substituting (12) into (5) results in the input admittance of the current-source inverter

$$Y_i(s) = \frac{1}{Z_i(s)} = \frac{A_{C21}(s)\frac{1}{Y_L(s)} + A_{C22}(s)}{A_{C11}(s)\frac{1}{Y_L(s)} + A_{C12}(s)} = Y_L(s) + Y_{Cs}(s), \quad (13)$$

where  $Y_L(s)$  and  $Y_{Cs}(s)$  are the load and source admittances, respectively, as shown in Fig. 4(b), while the input voltage of the current source is thus obtained as

$$V_{Cs}(s) = \frac{I_{Cs}(s)}{Y_L(s) + Y_{Cs}(s)}, \quad (14)$$

where  $I_{Cs}(s)$  is the current of the current source, as shown in Fig. 4(b).

An inverter normally includes at least one inverter bridge, and such a bridge is normally composed of one upper switch and one lower switch. On each bridge, either the upper or the lower switch must be kept on; otherwise, one has  $Y_L(s) = 0$ . Moreover, the source admittance  $Y_{Cs}(s)$  is normally very small, i.e.  $Y_{Cs}(s) \approx 0$ . Therefore,  $Y_i(s) = Y_L(s) + Y_{Cs}(s) \approx 0$ , which implies  $V_{Cs}(s) \rightarrow \infty$ . Thus, the current

source is open-circuit and a very large voltage will destroy the switches.

In order to prevent the open-circuit problem, the overlapped-time technique on upper and lower switches has normally been utilised to ensure at least one of the upper switches and one of the lower switches to be on at any time [47].

#### 3.2.2. Limited output-current gain

In terms of (6), one can obtain the output admittance of the current-source inverter as

$$Y_o(s) = \frac{1}{Z_o(s)} = \frac{A_{C21}(s)\frac{1}{Y_{Cs}(s)} + A_{C11}(s)}{A_{C22}(s)\frac{1}{Y_{Cs}(s)} + A_{C12}(s)} = Y_{Cs}(s), \quad (15)$$

while the output current is

$$I_{CL}(s) = I_{Cs}(s) - V_{Cs}(s)Y_{Cs}(s). \quad (16)$$

For  $V_{Cs}(s) \geq 0$  and  $Y_{Cs} \geq 0$ , one has  $I_{CL} \leq I_{Cs}$ , i.e. the load current  $I_{CL}(s)$  is lower than or equal to the source current  $I_{Cs}(s)$ .

#### 3.2.3. Inapplicability to inductive loads

The admittance  $Y_{Cs}(s)$  in a two-port network is equivalent to an inductor with very large inductance, which implies that  $Y_{Cs}(s) = -j\frac{1}{\omega L} \approx 0$ . It is remarked that if the load admittance  $Y_L(s)$  is inductive, an inductive source offers energy to an inductive load, while  $I_{CL}(s) = I_{Cs}(s)$  at a steady state implies that the current-source inverter does not work, and is thus inapplicable to inductive loads.

It is concluded that, due to the admittance of the two-port network between the current source and the inverter bridges, the current-source inverter has the problems of open-circuit, limited output-current gains and inapplicability to inductive loads.

## 4. Z-source inverters

Peng [21] proposed in 2002 to use an impedance-network (named Z-network), as shown in Fig. 5 and in the rectangles in Fig. 6, coupled with a DC source to form a novel source, including voltage- and

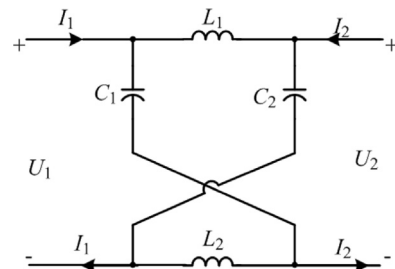


Fig. 5. A Z-network.

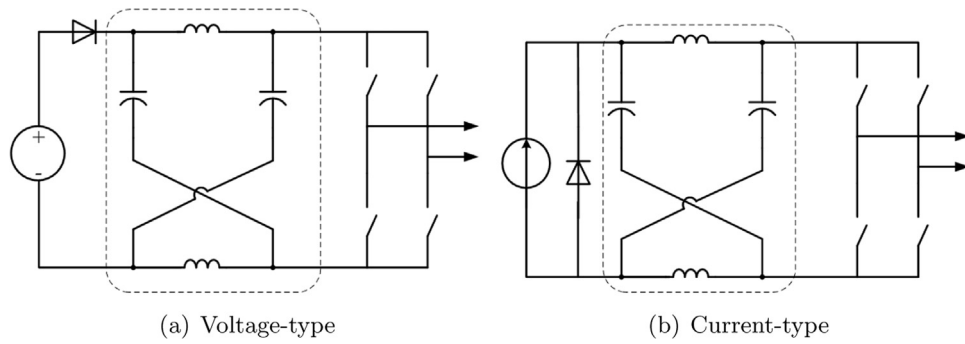


Fig. 6. Z-source inverters.

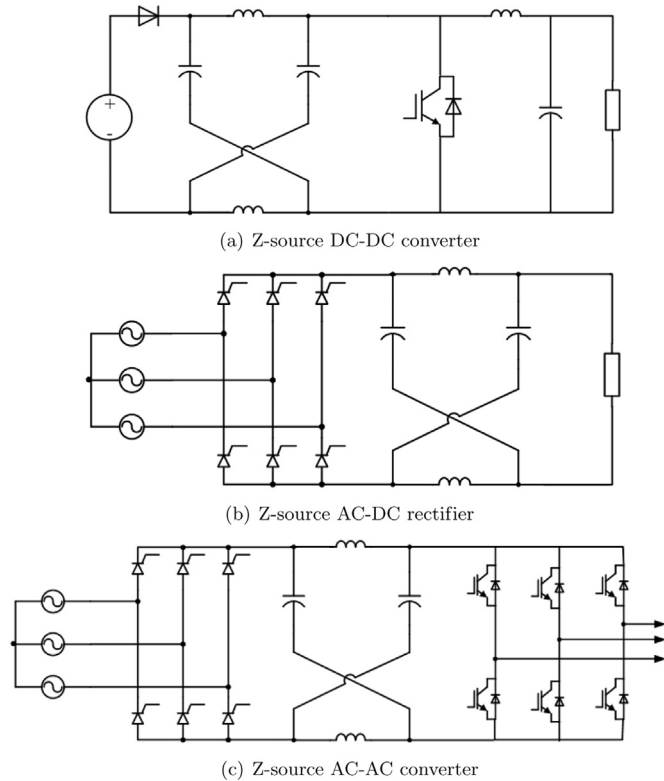


Fig. 7. Typical Z-source converters.

current-type Z-source inverters, as shown in Fig. 6. Applying this Z-source technique in other converters results in Z-source DC-DC converters (Fig. 7(a)), Z-source AC-DC rectifiers (Fig. 7(b)) and Z-source AC-AC converters (Fig. 7(c)).

Similarly and for simplicity, the voltage-type Z-source inverter is also taken as an example to explain the reasons why Z-source converters can overcome the problems of voltage-source and current-source converters. The diagram of a voltage-type Z-source inverter is drawn in Fig. 6(a), whose equivalent two-port network is illustrated in the dashed box in Fig. 8.

Assume  $L_1 = L_2 = L$  and  $C_1 = C_2 = C$ , and denote the impedance of diode  $D$  by  $Z_{ZS}(s)$ . In terms of (2), one can obtain the transmission matrix of the Z-network as

$$\mathbf{A}_Z(s) = \begin{bmatrix} A_{Z11}(s) & A_{Z12}(s) \\ A_{Z21}(s) & A_{Z22}(s) \end{bmatrix}, \quad (17)$$

where, in terms of (3), the elements read

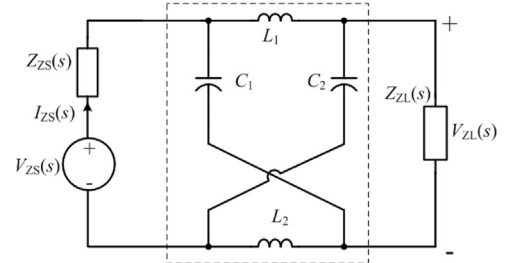


Fig. 8. Equivalent circuit of voltage-type Z-source inverters with two-port network.

$$\begin{cases} A_{Z11}(s) = \frac{1 + s^2LC}{1 - s^2LC}, \\ A_{Z12}(s) = \frac{2sL}{1 - s^2LC}, \\ A_{Z21}(s) = \frac{2sC}{1 - s^2LC}, \\ A_{Z22}(s) = \frac{1 + s^2LC}{1 - s^2LC}. \end{cases} \quad (18)$$

Substituting  $Z_S(s) = Z_{ZS}(s)$ ,  $Z_L(s) = Z_{ZL}(s)$  and (18) into (5) and (6) results in the input and output impedances of the Z-network as

$$\begin{cases} Z_{Zi}(s) = \frac{A_{Z11}(s)Z_{ZL}(s) + A_{Z12}(s)}{A_{Z21}(s)Z_{ZL}(s) + A_{Z22}(s)} = \frac{(s^2LC + 1)Z_{ZL}(s) + 2sL}{s^2LC + 2sCZ_{ZL}(s) + 1}, \\ Z_{Zo}(s) = \frac{A_{Z22}(s)Z_{ZS}(s) + A_{Z12}(s)}{A_{Z21}(s)Z_{ZS}(s) + A_{Z11}(s)} = \frac{(s^2LC + 1)Z_{ZS}(s) + 2sL}{s^2LC + 2sCZ_{ZS}(s) + 1}, \end{cases} \quad (19)$$

where  $Z_{ZS}(s)$  is the source impedance of the Z-network's input port and  $Z_{ZL}(s)$  is the load impedance of its output port described by

$$Z_{ZS}(s) = \begin{cases} 0, & \text{if } D \text{ is on,} \\ \infty, & \text{otherwise,} \end{cases} \quad (20)$$

and

$$Z_{ZL}(s) = \begin{cases} 0, & \text{at a shoot-through state,} \\ \infty, & \text{at an open-circuit state,} \\ Z_Z(s), & \text{otherwise,} \end{cases} \quad (21)$$

where  $Z_Z(s)$  is the load impedance of the inverter bridge. Substituting (20) and (21) into (19) leads to the input and output impedances as

$$Z_{Zi}(s) = \begin{cases} \frac{2sL}{s^2LC + 1}, & \text{at a shoot-through state,} \\ \frac{s^2LC + 1}{2sC}, & \text{at an open-circuit state,} \\ \frac{(s^2LC + 1)Z_Z(s) + 2sL}{2sCZ_Z(s) + s^2LC + 1}, & \text{otherwise,} \end{cases} \quad (22)$$

and

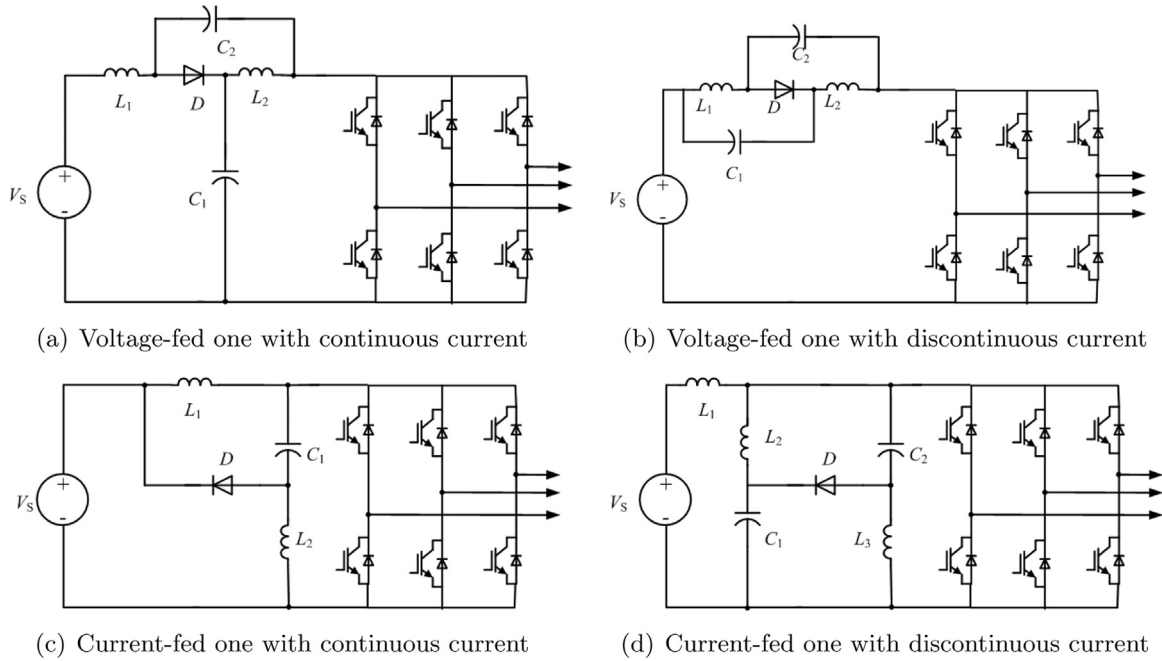


Fig. 9. Quasi-Z-source inverters [59].

$$Z_{zo}(s) = \begin{cases} \frac{2sL}{s^2LC + 1}, & \text{if } D \text{ is on,} \\ \frac{s^2LC + 1}{2sC}, & \text{otherwise.} \end{cases} \quad (23)$$

#### 4.1. Immunity to shoot-through

The input current of the Z-source inverter is expressed as

$$I_{zs}(s) = \frac{V_{zs}(s)}{Z_{zi}(s)}, \quad (24)$$

where  $Z_{zl}(s) = 0$  when the switches on a bridge are turned on simultaneously. It is obvious that  $Z_{zi}(s) \neq 0$  holds in all cases in terms of (22). Therefore, shoot-through will not happen for the Z-source inverter. Compared to the voltage-source inverter, the Z-source inverter is immune to the shoot-through problem, so that the short-circuit phenomenon at the source can be avoided, because the Z-network increases the input impedance.

#### 4.2. High output-voltage gain

Denote the duty cycle of the diode  $D$  as  $d$  and assume  $d \in [0, 1]$ . In terms of (23), one can obtain the average output impedance as

$$Z_{zo}(s) = \frac{(1-d)L}{2} \left( \frac{s^4 + s^2 \left( \frac{2(1+d)}{(1-d)LC} \right) + \frac{1}{L^2C^2}}{s^3 + s \frac{1}{LC}} \right), \quad (25)$$

while the output voltage of the Z-source inverter,  $V_{zl}(s)$ , is expressed as

$$V_{zl}(s) = V_{zs}(s) - I_{zl}(s)Z_{zo}(s). \quad (26)$$

It is obvious that  $Z_{zo}(s)$  is a function of the duty  $d$  in terms of (25). Adjusting  $Z_{zo}(s)$  to be negative or positive via  $d$ , one can obtain either  $V_{zl}(s) > V_{zs}(s)$  or  $V_{zl}(s) < V_{zs}(s)$  at will, which implies that Z-source inverters can overcome the problem of limited voltage gains which traditional voltage-source inverters have.

#### 4.3. Applicability both to capacitive and inductive loads

Assume that  $Z_z(s)$  is capacitive. Then, in terms of (23), one has

$$Z_z(s) = \frac{1}{sC_L}, \quad (27)$$

where  $C_L$  is the capacitance of the load. By adjusting the duty cycle  $d$ , the inductance  $L$  and capacitance  $C$  of the Z-network, its output impedance can exhibit the inductive feature, implying that the Z-source inverter is applicable to a capacitive load. Similarly, assume that  $Z_z(s)$  is inductive, then one can also prove that the Z-source inverter is also applicable to an inductive load.

It is thus concluded that, due to the embedded Z-network, Z-source inverters have unique advantages over traditional ones, i.e. immunity to shoot-through, higher output-voltage gains and applicability both to capacitive and inductive loads, which open up great potential in renewable energy applications.

### 5. State of the art of impedance-source converters

Inspired by the typical Z-source converter proposed by Peng, various impedance-source converters have been proposed for different applications, such as quasi-Z-source converters, trans-Z-source converters or embedded-Z-source converters. So far, more than 1100 articles on impedance-source converters have been published in various professional journals by many scholars [22–26], e.g. by Peng [49], Loh [50–53], Tang [54,55], Jung [56], Varjani [57,36] and Vinnikov [58]. Some typical Z-source converters are to be reviewed in this section.

#### 5.1. Quasi-Z-source converters

The quasi-Z-source converter was proposed by Anderson and Peng in 2008 for applications in motor systems, renewable energy systems and micro-grid systems. According to the operational modes voltage-type or current-type and continuous or discontinuous current, quasi-Z-source converters can be classified into four categories, i.e. voltage-fed quasi-Z-source inverters with continuous input current, voltage-fed quasi-Z-source inverters with discontinuous input current, current-fed quasi-Z-source inverters with continuous input current and current-fed

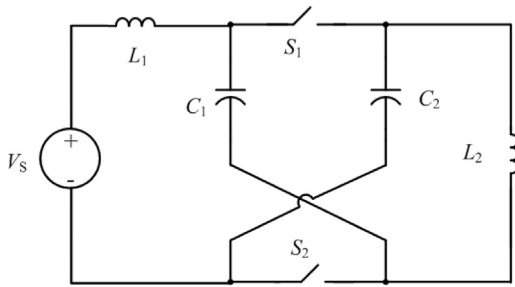


Fig. 10. Equivalent circuit of the converter in Fig. 9 [60].

quasi-Z-source inverters with discontinuous input current, which are shown in Fig. 9 [59]. It was found by Cao and Peng [60] that all impedance-networks in Fig. 9 can be derived from the one in Fig. 5. For instance, the voltage-fed quasi-Z-source inverter with continuous input current in Fig. 9(a) is equivalent to that in Fig. 10, whose switches  $S_1$  and  $S_2$  are equivalent to the diode  $D$  and the inverting bridge in Fig. 9(a), respectively.

It is remarked that the impedance-network in Fig. 10 is a typical quasi-Z-network, based on which various quasi-Z-networks can be derived. For example, Cao and Peng have proposed a family of quasi-Z-source DC-DC converters [60], and Vinnikov et al. have also proposed some novel quasi-Z-source DC-DC converters for renewable energy systems [61].

### 5.2. Trans-Z-source converters

Compared with traditional voltage-source converters, whose voltage gains are normally in the scale of 5~6, typical Z-source and quasi-Z-source converters can reach much higher voltage gains in the scale of 20, which are, however, still not big enough for some special applications. For example, voltage gains of converters utilised in solar energy systems need to reach the scales of decades or even hundreds.

In 2010, Qian and Peng et al. have integrated the transformers or coupled inductors into Z-networks (shown in Fig. 5) and quasi-Z-networks (shown in Fig. 10) to construct trans-Z-networks (shown in the dashed box in Fig. 11) [62] and to coin various trans-Z-source converters.

In terms of different operational modes of input current and coupled inductors, trans-Z-source converters can be classified into six categories, viz. voltage-fed trans-quasi-Z-source inverters, current-fed trans-quasi-Z-source inverters, voltage-fed trans-quasi-Z-source inverters with coupled inductors, current-fed trans-quasi-Z-source inverters with two coupled inductors, voltage-fed trans-Z-source inverters and current-fed trans-Z-source inverters, as shown in Fig. 11. Therein, trans-Z-source converters not only maintain the main features of traditional Z-source converters, but also exhibit some unique advantages, namely increased voltage gains and reduced voltage stress for the voltage-fed trans-Z-source inverters due to the transformers or coupled inductors, and an expanded operation quadrant for the current-fed trans-Z-source inverters. However, transformers and coupled inductors increase volume and cost.

### 5.3. Embedded-Z-source converters

In order to obtain smaller volume and higher robustness, in 2010 Loh et al. proposed embedded-Z-source converters [63]. Instead of using an external LC filter, they proposed an alternative family of embedded-Z-source inverters, which adopts the concept of embedding the input DC sources into the LC impedance-network, using its existing inductive elements for current filtering in voltage-type embedded-Z-source inverters, and its capacitive elements for voltage filtering in current-type embedded-Z-source inverters. The typical

topologies can be classified into a two-level type and a three-level type, as shown in Fig. 12.

It is remarked that the embedded-Z-source inverters do not only maintain the features of typical Z-source inverters, but also generate smaller ripples of input voltage and current.

### 5.4. Other impedance-source converters

In addition to the above-mentioned impedance-source converters, some others have also been proposed, like Y-source converters (Fig. 13) [64],  $\Gamma$ -Z-source converters (Fig. 14) [65–68], LCCT-Z-source converters (Fig. 15) [69,70] and Z-H-source converters (Fig. 16) [71], to list just a few.

Y-source converters as shown in Fig. 13 are designed on the basis of trans-Z-source converters which, however, realise a higher voltage gain by using a smaller duty ratio.

The  $\Gamma$ -Z-source converters shown in Fig. 14 are essentially derived from trans-Z-source converters. They use fewer components and a coupled transformer to provide a high voltage gain. Two  $\Gamma$ -shaped inductors (Fig. 14(a)) are coupled in trans-Z-source converters to form  $\Gamma$ -Z-source converters. Moreover, a voltage source embedded in the  $\Gamma$ -shaped network in Fig. 14(a) yields an embedded-Z-source converter.

With LCCT standing for inductor-capacitor-capacitor-transformer, the LCCT-Z-source converters shown in Fig. 15 are extensions of trans-Z-source inverters with unique features, such as the converter in Fig. 15(b), whose two built-in DC blocking capacitors, cascaded with transformer windings, can prevent the transformer from saturation, while the one in Fig. 15(a), whose built-in DC capacitor (or electrolytic capacitor), cascaded with transformer windings, possesses the features of both quasi-Z-source and trans-Z-source converters.

Fig. 16 depicts a Z-H-source converter, which contains fewer components, but has the same functionality as traditional Z-source converters.

It is remarked that, so far, the design of an impedance-source converter is still an art, and cannot fulfill industrial requirements. The rapidly developing renewable-energy industry has posed higher and more stringent requirements on power electronics, especially high-quality converters. Therefore, a systematic design methodology is desired. Owing to the important rôle of impedance-networks, coupled with traditional converters to construct impedance-source converters, it is significant to understand impedance-network matching, which lays a foundation for a systematic design methodology.

## 6. Impedance-network matching

### 6.1. Impedance matching

The concept of impedance matching deals originally with linear circuits, and is not directly applicable to power converters, where essentially nonlinear switched circuits prevail. Nevertheless, in each operational mode, a power converter works as a linear circuit, which results in the time-varying characteristics of impedance-network matching. Therefore, the concept of impedance matching can be extended to impedance-network matching in three aspects: input-impedance matching, output-impedance matching and load-phase matching.

### 6.2. Impedance-network matching

#### 6.2.1. Input-impedance matching

Substituting  $s = j\omega$  into the input impedance of the two-port network in (5) results in

$$Z_i(j\omega) = \operatorname{Re} \left( \frac{A_{11}(j\omega)Z_L(j\omega) + A_{12}(j\omega)}{A_{21}(j\omega)Z_L(j\omega) + A_{22}(j\omega)} \right) + j \operatorname{Im} \left( \frac{A_{11}(j\omega)Z_L(j\omega) + A_{12}(j\omega)}{A_{21}(j\omega)Z_L(j\omega) + A_{22}(j\omega)} \right). \quad (28)$$

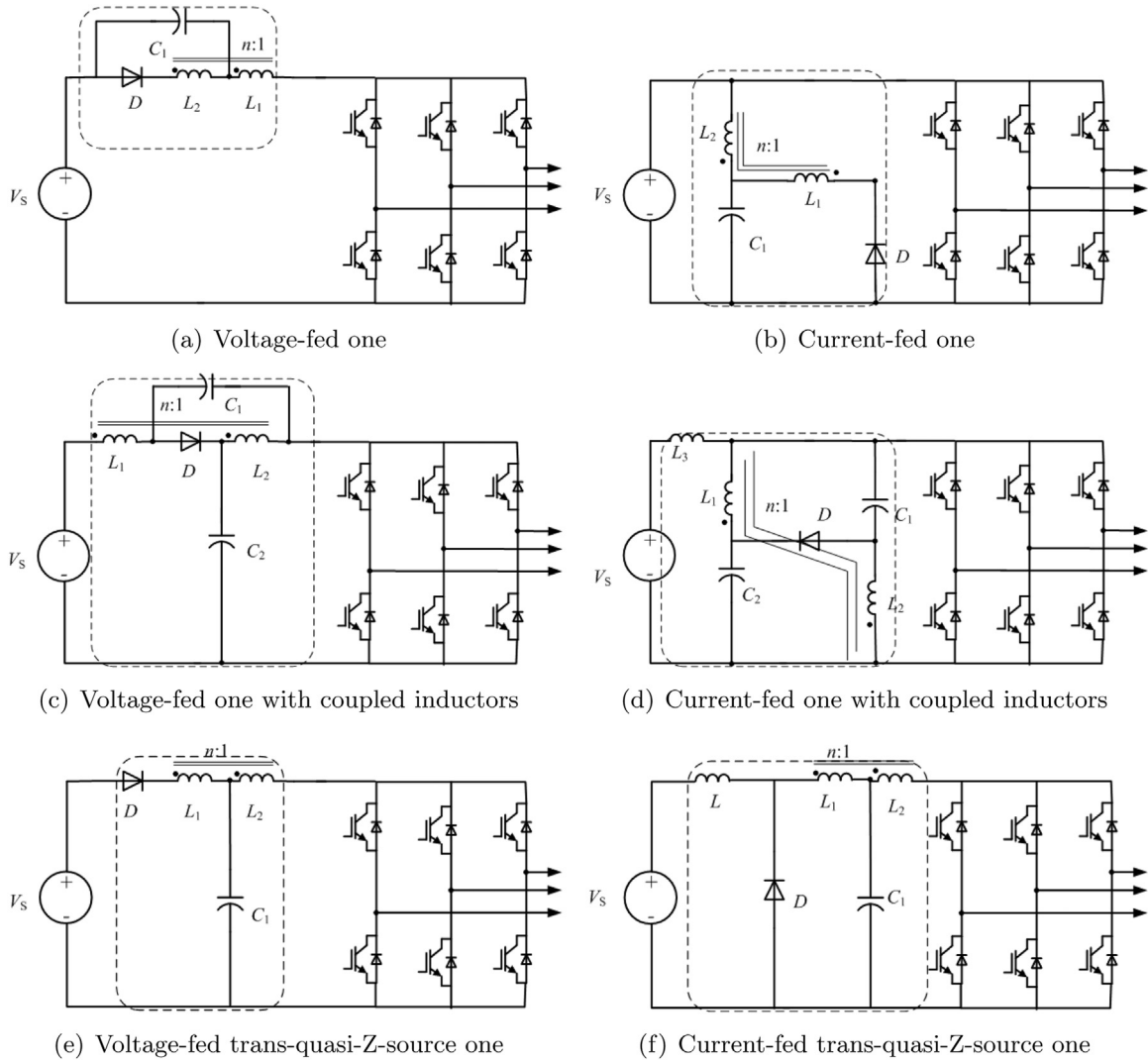


Fig. 11. Typical trans-Z-source converters [62].

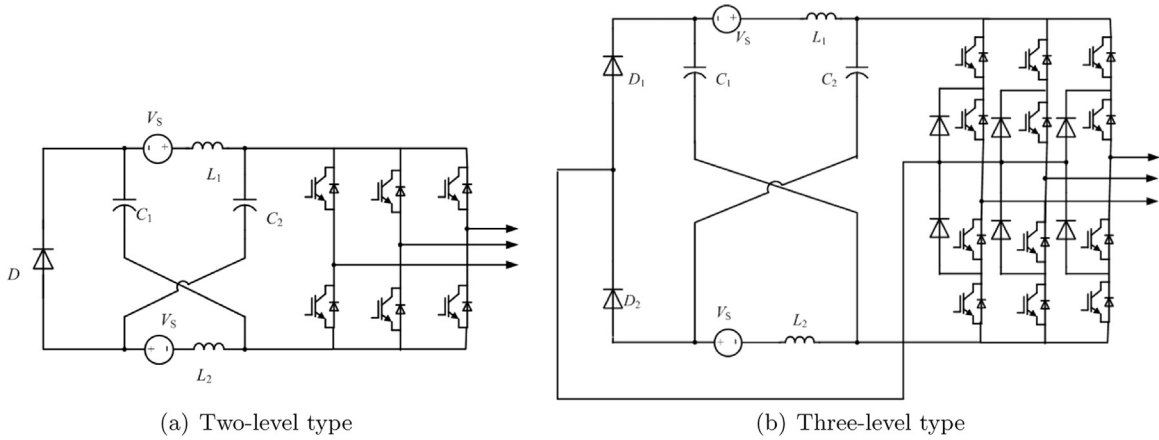


Fig. 12. Typical embedded-Z-source converters [63].

The shoot-through state implies that  $Z_L(j\omega) = 0$ , so the input impedance in shoot-through state is derived as

$$Z_i(j\omega) = \text{Re} \left( \frac{A_{12}(j\omega)}{A_{22}(j\omega)} \right) + j \text{Im} \left( \frac{A_{12}(j\omega)}{A_{22}(j\omega)} \right), \quad (29)$$

whereas the input current of the voltage source at shoot-through states is expressed as

$$I_s(j\omega) = \frac{V_s(j\omega)}{Z_i(j\omega)} = \frac{V_s(j\omega)}{\text{Re} \left( \frac{A_{12}(j\omega)}{A_{22}(j\omega)} \right) + j \text{Im} \left( \frac{A_{12}(j\omega)}{A_{22}(j\omega)} \right)}. \quad (30)$$

Since inductive components hinder their current to change, it is then obvious that the converter can restrain the short-circuit current if its input impedance in (29) is inductive.

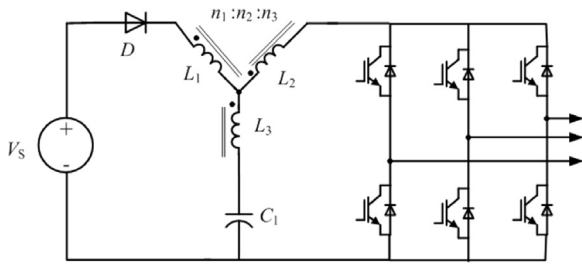


Fig. 13. Y-source converters [64].

$$\text{Im}\left(\frac{A_{12}(j\omega)}{A_{22}(j\omega)}\right) > 0. \quad (31)$$

### 6.2.2. Output-Impedance matching

Substituting  $s = j\omega$  into the output voltage equation  $V_L(s) = V_S(s) - I_L(s)Z_o(s)$  results in  $V_L(j\omega) = V_S(j\omega) - I_L(j\omega)Z_o(j\omega)$ . It is remarked that in order for the output voltage to be higher than the source voltage, the output impedance  $Z_o(j\omega)$  should be negative; otherwise, the output impedance  $Z_o(j\omega)$  should be positive.

Substituting  $s = j\omega$  into (6) leads to the output impedance of the two-port network as

$$Z_o(j\omega) = \text{Re}\left(\frac{A_{22}(j\omega)Z_S(j\omega) + A_{12}(j\omega)}{A_{21}(j\omega)Z_S(j\omega) + A_{11}(j\omega)}\right) + j\text{Im}\left(\frac{A_{22}(j\omega)Z_S(j\omega) + A_{12}(j\omega)}{A_{21}(j\omega)Z_S(j\omega) + A_{11}(j\omega)}\right), \quad (32)$$

while the corresponding output voltage is

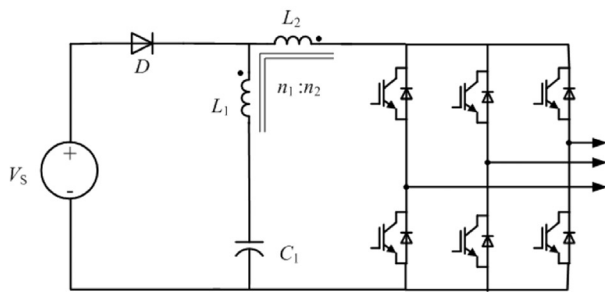
$$V_L(j\omega) = V_S(j\omega) \frac{Z_L(j\omega)}{Z_L(j\omega) + Z_o(j\omega)}. \quad (33)$$

It is obvious that  $|V_L(j\omega)| > |V_S(j\omega)|$ , if the voltage gain  $M$  satisfies the condition  $M > 1$ , namely,

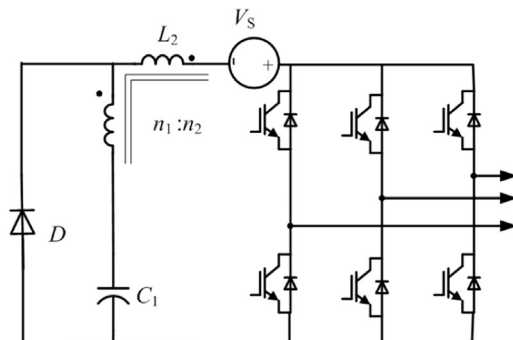
$$\begin{aligned} M &= \frac{|V_L(j\omega)|}{|V_S(j\omega)|} \\ &= \left| \frac{Z_L(j\omega)}{Z_L(j\omega) + Z_o(j\omega)} \right| \\ &= \frac{|Z_L(j\omega)|}{|Z_L(j\omega) + Z_o(j\omega)|} \\ &= \frac{\sqrt{[\text{Re}(Z_L(j\omega))]^2 + [\text{Im}(Z_L(j\omega))]^2}}{\sqrt{[\text{Re}(Z_L(j\omega)) + \text{Re}(Z_o(j\omega))]^2 + [\text{Im}(Z_L(j\omega)) + \text{Im}(Z_o(j\omega))]^2}} > 1, \end{aligned} \quad (34)$$

from which one has

$$\begin{aligned} [\text{Re}(Z_L(j\omega))]^2 + [\text{Im}(Z_L(j\omega))]^2 &> [\text{Re}(Z_L(j\omega)) + \text{Re}(Z_o(j\omega))]^2 \\ &+ [\text{Im}(Z_L(j\omega)) + \text{Im}(Z_o(j\omega))]^2, \end{aligned} \quad (35)$$



(a) Source placed in series with diode



(b) Source placed in series with inverter bridge

Fig. 14. Γ-Z-source converters [65].

which can be further simplified as

$$\begin{aligned} 2[\text{Re}(Z_L(j\omega))\text{Re}(Z_o(j\omega)) + \text{Im}(Z_L(j\omega))\text{Im}(Z_o(j\omega))] &+ [\text{Re}(Z_o(j\omega))]^2 \\ &+ [\text{Im}(Z_o(j\omega))]^2 = 2[\text{Re}(Z_L(j\omega))\text{Re}(Z_o(j\omega)) \\ &+ \text{Im}(Z_L(j\omega))\text{Im}(Z_o(j\omega))] + |Z_o(j\omega)|^2 < 0. \end{aligned} \quad (36)$$

If one has

$$\text{Re}(Z_L(j\omega))\text{Re}(Z_o(j\omega)) + \text{Im}(Z_L(j\omega))\text{Im}(Z_o(j\omega)) < -\frac{|Z_o(j\omega)|^2}{2} < 0, \quad (37)$$

then (34) holds. That is, if  $\text{Re}(Z_L(j\omega))\text{Re}(Z_o(j\omega)) < 0$  or  $\text{Im}(Z_L(j\omega))\text{Im}(Z_o(j\omega)) < 0$ , and their sum is smaller than 0, then (37) holds. Moreover, (37) suggests that the real parts of the load impedance and the output impedance should have opposite signs, or the imaginary parts of the load impedance and the output impedance should have opposite signs. This means that the output impedance should have negative impedance features; otherwise, the output impedance exhibits positive impedance features.

### 6.2.3. Load-phase matching

In order to improve an inverter's load ability, so that it becomes applicable to both inductive and capacitive loads, the inverter's output impedance phase should be capacitive or inductive so as to match the load impedance to reduce the inverter's impedance phase angle. Therein, the total impedance phase is the sum of the output-impedance phase and load-impedance phase. Moreover, the smaller the total impedance phase is, the larger is the inverter's power factor. Therefore, the optimal condition is its total impedance phase to be  $0^\circ$ .

The impedance-phase angle of the converter is given by

$$\varphi = \arctan\left(\frac{\text{Im}(Z_o(j\omega) + Z_L(j\omega))}{\text{Re}(Z_o(j\omega) + Z_L(j\omega))}\right). \quad (38)$$

In terms of (32),

$$\text{Im}(Z_o(j\omega) + Z_L(j\omega)) = \text{Im}\left(\frac{A_{22}(j\omega)Z_S(j\omega) + A_{12}(j\omega)}{A_{21}(j\omega)Z_S(j\omega) + A_{11}(j\omega)} + Z_L(j\omega)\right) = 0 \quad (39)$$

implies that its impedance-phase angle is  $0^\circ$ . Moreover, (39) can be further simplified to

$$\text{Im}(Z_L(j\omega)) = -\text{Im}(Z_o(j\omega)) = -\text{Im}\left(\frac{A_{22}(j\omega)Z_S(j\omega) + A_{12}(j\omega)}{A_{21}(j\omega)Z_S(j\omega) + A_{11}(j\omega)}\right). \quad (40)$$

### 6.3. Matching practice

It is now known that input-impedance matching is to increase the input impedance for the short-circuit case, so that the input impedance becomes inductive and also restrains the input current. Output-impedance matching is to tune the output impedance to be of positive or negative nature, so as to increase or decrease the output voltage by

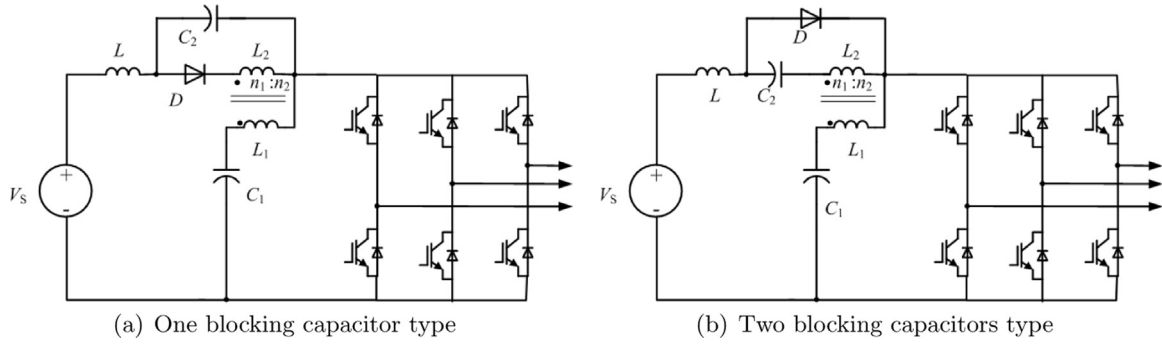


Fig. 15. LCCT-Z-source converters [69].

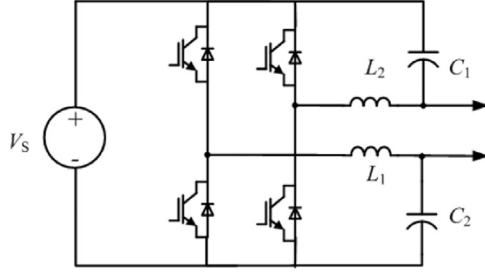


Fig. 16. Z-H-source converters [71].

connecting an impedance-network or adjusting the impedance-networks' parameters. Finally, load-phase matching is to match the output impedance with the load impedance to ensure the impedance-phase angle to be  $0^\circ$ , so that the energy-transmission efficiency is optimised. Hence, in designing an impedance-source converter, input-impedance matching, output-impedance matching and load-phase matching should be considered together.

From Sections 6.2.1–6.2.3, criteria for impedance-network matching can be concluded as

$$\begin{cases} \operatorname{Im}\left(\frac{A_{12}(j\omega)}{A_{22}(j\omega)}\right) > 0, \\ \operatorname{Re}(Z_L(j\omega))\operatorname{Re}(Z_o(j\omega)) + \operatorname{Im}(Z_L(j\omega))\operatorname{Im}(Z_o(j\omega)) < -\frac{|Z_o(j\omega)|^2}{2}, \\ \operatorname{Im}(Z_L(j\omega)) = -\operatorname{Im}\left(\frac{A_{22}(j\omega)Z_S(j\omega) + A_{12}(j\omega)}{A_{21}(j\omega)Z_S(j\omega) + A_{11}(j\omega)}\right). \end{cases} \quad (41)$$

Thus, to design an impedance-source converter is to determine the topologies and parameters of the impedance-network, the source impedance and the load impedance, so that (41) is satisfied, which is to be concretised in the next section.

## 7. Design methodology

### 7.1. Topology design

Determining the performance of converters, the topology of impedance-networks deals with impedance-network connectivity and component locations.

#### 7.1.1. Impedance-network connectivity

Impedance-network connectivity refers to the terminals' connectivity of two impedance-networks. There are four terminals in each impedance-network, which results in different connectivity types of two-port networks, i.e. cascade, parallel, series-parallel, parallel-series and series-series connectivities, as well as the corresponding operational rules shown in Table 1.

Therein, **A**, **Y**, **H**, **G** and **Z** are the matrices of transmission parameter, admittance parameters, hybrid parameters, inverse hybrid

parameters and impedance parameters, respectively. Moreover, the connectivity of two-port networks as shown in Table 1 can be the connectivity between two impedance-networks, between an impedance-network and the source, or between an impedance-network and a load.

#### 7.1.2. Location of an impedance-network

The location of an impedance-network can be varied.

1. As shown in Fig. 17(a), the impedance-network can be placed between the source and a part of the converter, e.g. illustrated in Figs. 6, 7(a), 9, 11, 13, 14(a) and 15.
2. As shown in Fig. 17(b), the impedance-network can be placed inside the converter, e.g. the Z-source AC-AC converter in Fig. 7(c).
3. As shown in Fig. 17(c), the impedance-network can be placed between the converter and the load, e.g. the Z-source AC-DC converter in Fig. 7(b) and the Z-H-source converter in Fig. 16.

### 7.2. Selection of an impedance-network

Basic two-port impedance-networks and their transmission parameters matrices are listed in Table 2, where  $Z_x = Z_1Z_2Z_3Z_4$ .

Denote the source impedance in the input port of the two-port network as  $Z_{2S}$  and the load impedance in its output port as  $Z_{2L}$ , then the corresponding input and output impedances can be expressed in terms of (5) and (6) as listed in Table 3. Moreover, the impedance-phase angle of the two-port impedance-network is given as

$$\varphi = \arctan\left(\frac{\operatorname{Im}(Z_o + Z_{2L})}{\operatorname{Re}(Z_o + Z_{2L})}\right). \quad (42)$$

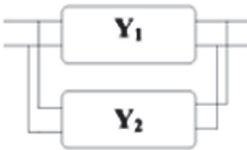
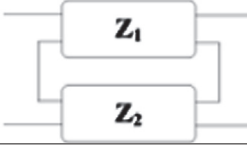
Substituting the output impedance  $Z_o$  in Table 3 into (42) results in the corresponding impedance-phase angles, which helps to select proper impedance-networks. It is remarked that

1.  $Z_{Xi} = \frac{(Z_x + Z_1Z_3 + Z_2Z_4 + 1)Z_{2L} + Z_1Z_2Z_4 + Z_1Z_3Z_4 + Z_1 + Z_4}{(Z_1Z_2Z_3 + Z_2Z_3Z_4 + Z_2 + Z_3)Z_{2L} + Z_1Z_2 + Z_3Z_4 + Z_x + 1}$ ,
2.  $Z_{Xo} = \frac{(Z_x + Z_1Z_2 + Z_3Z_4 + 1)Z_{2S} + Z_1Z_2Z_4 + Z_1Z_3Z_4 + Z_1 + Z_4}{(Z_1Z_2Z_3 + Z_2Z_3Z_4 + Z_2 + Z_3)Z_{2S} + Z_1Z_2 + Z_3Z_4 + Z_x + 1}$ ,
3.  $Z_T = Z_1Z_2 + Z_1Z_3 + Z_2Z_3$ .

### 7.3. Input-impedance

In different operational modes a power converter works as different linear circuits, which leads to the time-varying characteristics of impedance matching. Three cases of power converters, i.e. short-circuit, open-circuit and normal operation, correspond to three input-impedance cases of a two-port network. In the short-circuit case, the output port of the two-port network is short-circuited, and its input-impedance is  $Z_{is} = Z_{i|Z_{2L}=0}$ . Similarly, the open-circuit case refers to the situation of the two-port network's output port being open-circuit with its input-impedance reading  $Z_{io} = Z_{i|Z_{2L}=\infty}$ . Further, the input impedance of the two-port network in the normal case refers to

**Table 1**  
Connectivities of two-port networks and operational rules.

Type	Connectivity	Operations
Cascade		$A = A_1 A_2$
Parallel		$Y = Y_1 + Y_2$
Series-parallel		$H = H_1 + H_2$
Parallel-series		$G = G_1 + G_2$
Series-series		$Z = Z_1 + Z_2$

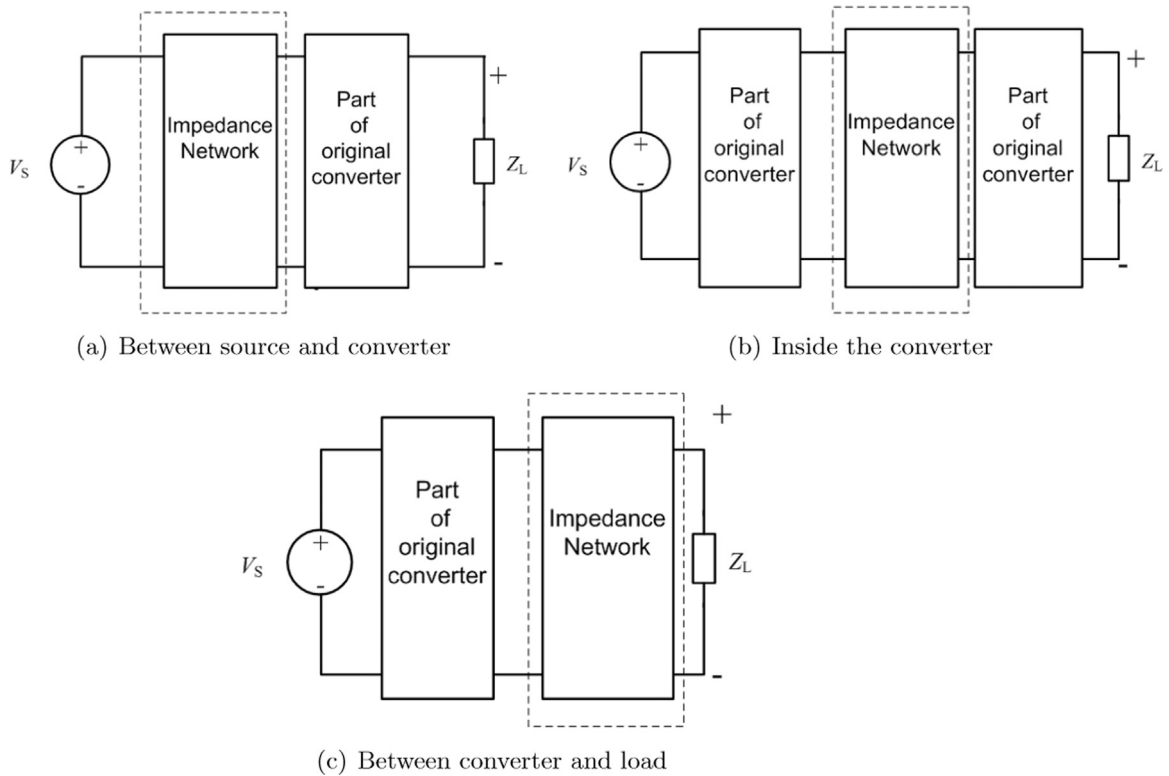


**Fig. 17.** Location of an impedance-network in converters.

**Table 2**  
Basic two-port impedance-networks and their transmission parameters matrices.

Networks type	Figure	Transmission matrix <b>A</b>
Basic cascaded		$\begin{bmatrix} 1 & Z_1 \\ 0 & 1 \end{bmatrix}$
Basic paralleled		$\begin{bmatrix} 1 & 0 \\ \frac{1}{Z_1} & 1 \end{bmatrix}$
X-shaped		$\begin{bmatrix} \frac{Z_x + Z_1 Z_3 + Z_2 Z_4 + 1}{1 - Z_x} & \frac{Z_1 Z_2 Z_4 + Z_1 Z_3 Z_4 + Z_1 + Z_4}{1 - Z_x} \\ \frac{Z_1 Z_2 Z_3 + Z_2 Z_3 Z_4 + Z_2 + Z_3}{1 - Z_x} & \frac{Z_x + Z_1 Z_2 + Z_3 Z_4 + 1}{1 - Z_x} \end{bmatrix}$
$\pi$ -shaped		$\begin{bmatrix} \frac{Z_1 + Z_3}{Z_2 Z_3} & \frac{Z_1}{Z_2} \\ \frac{Z_1 + Z_2 + Z_3}{Z_2 Z_3} & \frac{Z_1 + Z_2}{Z_2} \end{bmatrix}$
$\Gamma$ -shaped		$\begin{bmatrix} 1 & Z_1 \\ \frac{1}{Z_2} & \frac{Z_1 + Z_2}{Z_2} \end{bmatrix}$
Inverse- $\Gamma$ -shaped		$\begin{bmatrix} \frac{Z_1 + Z_2}{Z_2} & Z_1 \\ \frac{1}{Z_2} & 1 \end{bmatrix}$
T-shaped		$\begin{bmatrix} \frac{Z_1 + Z_2}{Z_2} & \frac{Z_1 Z_2 + Z_1 Z_3 + Z_2 Z_3}{Z_2} \\ \frac{1}{Z_2} & \frac{Z_3 + Z_2}{Z_2} \end{bmatrix}$

**Table 3**  
Input- and output-impedances of two-port networks.

Networks types	$Z_i$	$Z_o$
Basic cascaded	$Z_{2L} + Z_1$	$Z_{2S} + Z_1$
Basic paralleled	$\frac{Z_{2L} Z_1}{Z_{2L} + Z_1}$	$\frac{Z_{2S} Z_1}{Z_{2S} + Z_1}$
X-shaped	$Z_{Xi}$	$Z_{Xo}$
$\pi$ -shaped	$\frac{(Z_1 + Z_3)Z_2 Z_{2L} + Z_1 Z_2 Z_3}{(Z_1 + Z_2 + Z_3)Z_{2L} + (Z_1 + Z_2)Z_3}$	$\frac{(Z_1 + Z_2)Z_3 Z_{2S} + Z_1 Z_2 Z_3}{(Z_1 + Z_2 + Z_3)Z_{2S} + (Z_1 + Z_3)Z_2}$
$\Gamma$ -shaped	$\frac{Z_2 Z_{2L} + Z_1 Z_2}{Z_{2L} + Z_1 + Z_2}$	$\frac{(Z_1 + Z_2)Z_{2S} + Z_1}{Z_{2S} + Z_4 + Z_2}$
Inverse- $\Gamma$ -shaped	$\frac{(Z_1 + Z_2)Z_{2L} + Z_1}{Z_{2L} + Z_4 + Z_2}$	$\frac{Z_2 Z_{2S} + Z_1 Z_2}{Z_{2S} + Z_1 + Z_2}$
T-shaped	$\frac{(Z_1 + Z_2)Z_{2L} + Z_1}{Z_{2L} + Z_2 + Z_3}$	$\frac{(Z_3 + Z_2)Z_{2S} + Z_1}{Z_{2S} + Z_2 + Z_1}$

$Z_{ic} = Z_i$ . For various cases the input-impedances are summarised in Table 4.

7.3.1. Short-circuit case

According to Table 4 it is straightforward that the input-impedance of the basic parallel type is 0 in the short-circuit case, implying the inability to prevent the short-circuit case; while the basic cascaded type

**Table 4**  
Input-impedances of two-port networks in different cases.

Networks types	Short-circuit case $Z_{is}$	Open-circuit case $Z_{io}$
Basic cascaded	$Z_1$	$\infty$
Basic paralleled	0	$Z_1$
X-shaped	$\frac{Z_1 Z_2 Z_4 + Z_1 Z_3 Z_4 + Z_1 + Z_4}{Z_1 Z_2 + Z_3 Z_4 + Z_1 Z_2 Z_3 Z_4 + 1}$	$\frac{Z_1 Z_3 + Z_2 Z_4 + Z_1 Z_2 Z_3 Z_4 + 1}{Z_1 Z_2 Z_3 + Z_2 Z_3 Z_4 + Z_2 + Z_3}$
$\pi$ -shaped	$\frac{Z_1 Z_2}{Z_1 + Z_2}$	$\frac{(Z_1 + Z_3)Z_2}{Z_1 + Z_2 + Z_3}$
$\Gamma$ -shaped	$\frac{Z_1 Z_2}{Z_1 + Z_2}$	$Z_2$
Inverse- $\Gamma$ -shaped	$\frac{Z_1}{Z_2}$	$Z_1 + Z_2$
T-shaped	$\frac{Z_1 Z_2 + Z_1 Z_3 + Z_2 Z_3}{Z_2 + Z_3}$	$Z_1 + Z_2$

cannot prevent the short-circuit case either when  $Z_1$  is very small, i.e. the voltage-source inverter is also a typical cascaded type, but it cannot prevent the short-circuit case as  $Z_1$  is close to 0.

7.3.2. Open-circuit case

From Table 4 it is obvious that the open-circuit input-impedance of the basic cascaded type is infinite, implying that it lacks the ability to

prevent the open-circuit case in the load, while the basic parallel type cannot prevent the open-circuit case either when  $Z_1 = \infty$ , i.e. the current-source inverter.

### 7.3.3. Normal case

For a converter operating in a normal case, its input-impedance of each two-port network is given in Table 3.

Normally, one can obtain the average input-impedance in one switching period with the corresponding control strategy as

$$Z_i = d_1 Z_{is} + d_2 Z_{io} + (1 - d_1 - d_2) Z_{ic}, \quad (43)$$

where  $d_1, d_2$  and  $1 - d_1 - d_2$  are the corresponding duty cycles of input-impedances in three cases, respectively.

### 7.4. Output-impedance

Similarly, the output-impedances of the two-port network can be obtained for the three cases as follows.

Case 1:  $Z_{2S} = 0$

Suppose that the input port of the two-port network is connected with an ideal voltage source, i.e.  $Z_{os} = Z_o|_{Z_{2S}=0}$ . Substituting  $Z_{2S} = 0$  into the equations for the output-impedance in Table 3 results in the corresponding output-impedances in Table 5.

In terms of Table 5 is the output-impedance of the basic cascade type in this case  $Z_1$ , and  $Z_1$  determines the features of the output-impedance, which lead to low output voltage, e.g. of the voltage-source inverter in Fig. 3(b), where  $Z_1 = Z_s$ . It is obvious that the output voltage is lower than the input voltage due to the output-impedance, and it can load the inductive loads, only.

Case 2:  $Z_{2S} \rightarrow \infty$

Suppose that the input port of the two-port network is open-circuit, i.e.  $Z_{oo} = Z_o|_{Z_{2S}=\infty}$ . Substituting  $Z_{2S} = \infty$  into the equations for the output-impedance in Table 3 leads to the corresponding output-impedances, given in Table 5.

Case 3: Normal case

Denote the output-impedance in the normal case as  $Z_{oc}$  in Table 3. It is remarked that the average output-impedance in one switching period is given by

$$Z_o = d_3 Z_{os} + d_4 Z_{oo} + (1 - d_3 - d_4) Z_{oc}, \quad (44)$$

where  $d_3, d_4$  and  $1 - d_3 - d_4$  are the corresponding duty cycles of input-impedances in three cases, respectively.

Similarly, the impedance phase of a converter can be obtained according to Table 5 and (42). Then, input-impedance matching, output-impedance matching and load-phase matching are comprehensively analysed to realise optimised matching.

### 7.5. Analysis of the operational status

Power switches in a power converter lead to different kinds of operational modes, which should be analysed in detail to understand

**Table 5**  
Output-impedances of two-port networks in different cases.

Networks type	$Z_{2S} = 0$	$Z_{2S} \rightarrow \infty$
Basic cascaded	$Z_1$	$\rightarrow \infty$
Basic paralleled	0	$Z_1$
X-shaped	$\frac{Z_1 Z_2 Z_4 + Z_1 Z_3 Z_4 + Z_1 + Z_4}{Z_1 Z_3 + Z_2 Z_4 + Z_1 Z_2 Z_3 Z_4 + 1}$	$\frac{Z_1 Z_2 + Z_3 Z_4 + Z_1 Z_2 Z_3 Z_4 + 1}{Z_1 Z_2 Z_3 + Z_2 Z_3 Z_4 + Z_2 + Z_3}$
$\pi$ -shaped	$\frac{Z_1 + Z_3}{Z_1 + Z_3}$	$\frac{(Z_1 + Z_2) Z_3}{Z_1 + Z_2 + Z_3}$
$\Gamma$ -shaped	$\frac{Z_1}{Z_2}$	$Z_1 + Z_2$
Inverse- $\Gamma$ -shaped	$\frac{Z_1 Z_2}{Z_1 + Z_2}$	$Z_2$
T-shaped	$\frac{Z_1 Z_2 + Z_1 Z_3 + Z_2 Z_3}{Z_2 + Z_1}$	$Z_3 + Z_2$

the overall performance of the converter. The analysis includes the energy-transfer process and deductions of voltage and current relationships through the law of conservation of energy, Kirchhoff's current and voltage laws and other basic circuit laws.

### 7.6. Parameters design

According to Section 7.5 and the impedance-matching conditions in (41), the parameters of the converter are determined via the transmission parameters' matrix.

### 7.7. Simulations and experiments

According to the parameters obtained in Section 7.6, simulations and experiments need to be conducted to verify the designed converters with circuit simulation software, e.g. MatLab/Simulink, PSIM or PSPICE.

## 8. Case study

### 8.1. A Z-source half-bridge converter

Electroplating is a kind of electrochemical process with the purpose to let metal ions cover the surface of negative electrodes evenly and smoothly. Owing to the non-uniformity of this solution, the DC voltage direction and the current density should be adjusted from time to time, which requires complicated designs for different products and processes [72,73]. With the rapid growth of the demand for electroplating products with very different voltages and duty cycles, there are increasingly stringent requirements on the electrochemical power supplies to provide a broad range of outputs, asymmetrical positive and negative voltages, step waves, recurrent pulses, square waves, triangular waves and saw-tooth waves [74].

In order to realise the aforementioned functions, the output voltages of electrochemical power supplies are required to be variable, including variable positive or negative output voltages and variable time ratios between positive and negative voltages. For instance, in order to realise smooth electroplating products, the current densities and directions should be varied according to the requirements of electroplating technology [72,73]. Traditionally, one had to compose several cascaded sub-circuits and to use complex control methods to generate an overlapped waveform of multi-output voltages [74,75], with the disadvantages that it is hard to control and regulate the output voltages and that the use of cascaded sub-circuits not only increases cost and size, but also leads to more complex, bulky structures and to system instabilities. Moreover, the corresponding converters had to be cascaded based on experience gained for different electroplating products. Therefore, traditional designs are made on a case-by-case basis and are dependent on expert experience, which cannot meet the requirements of industrial applications.

#### 8.1.1. System design

An impedance-network of the X-shaped two-port type as mentioned in Table 2 is chosen. Then, embedding the Z-network between the capacitors and the inverter bridge in the traditional half-bridge inverter results in the Z-source half-bridge converter as shown in Fig. 18.

Therein, an LC Z-network, consisting of capacitors  $C_1, C_2$  and inductors  $L_1, L_2$ , is integrated into a traditional half-bridge converter, consisting of capacitors  $C_{d1}, C_{d2}$ , switches  $S_1, S_2$  and diode  $D$ , which is used to prevent the current from flowing back to the source. Moreover, the inductors are employed in the Z-network to prevent strong currents in the circuit when the switches are in the shoot-through state [76].

#### 8.1.2. Experimental verification

To verify the feasibility and validity of the proposed converter, a

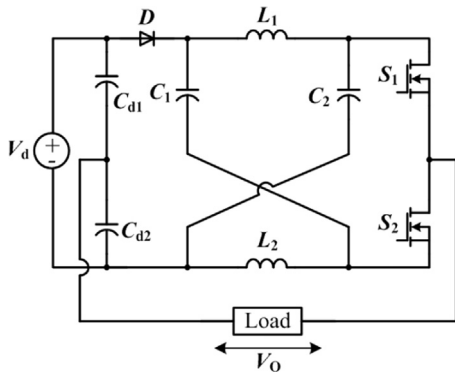


Fig. 18. Z-source half-bridge converter.

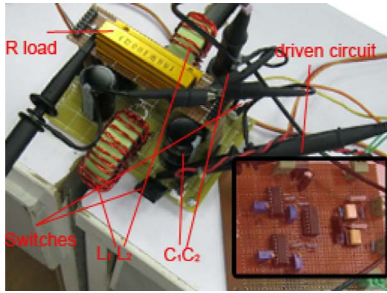


Fig. 19. Prototype of the proposed converter.

prototype of the Z-network converter was built as shown in Fig. 19, and the parameters were chosen as  $C_{d1} = C_{d2} = 470 \mu\text{F}$ ,  $C_1 = C_2 = 470 \mu\text{F}$ ,  $L_1 = L_2 = 100 \mu\text{H}$ ,  $R = 100 \Omega$  and  $T = 20 \mu\text{s}$ .

The waveforms of the converter's operation at  $d_1 = 0.5$  and  $d_2 = 0.7$  for the input voltage 40 V are shown in Fig. 20. Therein, the upper waveform refers to  $V_{GD}$  (Gate-Drain voltage) of the switch  $S_1$ , the middle one to  $V_{SD}$  (Source-Drain voltage) of the switch  $S_2$ , which is not, but can be synchronised to the driving waveform of  $S_2$ ; the lower waveform shows the output voltage of the load  $R$ , whose negative and positive output voltages are symmetric, and which are all about 50 V. This verifies the analytical and simulation results.

Fig. 21 depicts the experimental waveforms of the converter's operation for  $d_1 = 0.7$  and  $d_2 = 0.5$ . Therein, the negative and positive output voltages are asymmetric, the positive one is about 20 V, which is nearly equal to  $V_d/2$ , and the width is  $d_1T$ . The negative one is 40 V, which is much larger than  $V_d/2$ . The experimental results are also consistent with the simulation results.

### 8.2. A dual-output Z-source half-bridge converter

To reduce the number of power switches in hybrid electric vehicles (HEV) [77], a dual-output converter with nine switches is proposed in [57]. Therein, two inverters share three common switches, resulting in

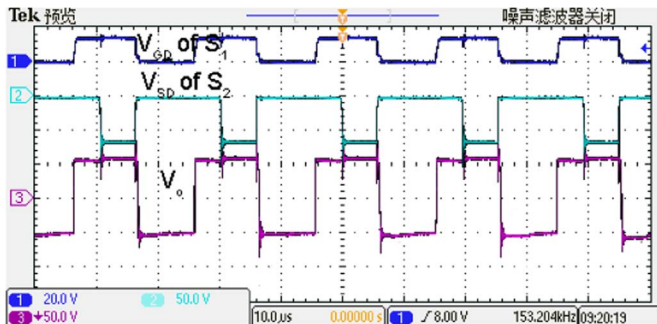


Fig. 20. Experimental waveforms in the shoot-through case ( $d_1 = 0.5$ ,  $d_2 = 0.7$ ).

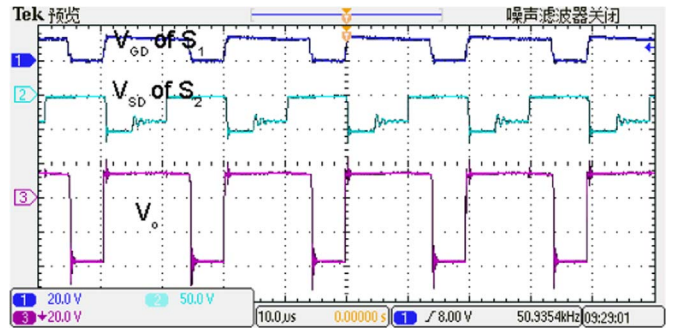


Fig. 21. Experimental waveforms in the shoot-through case ( $d_1 = 0.7$ ,  $d_2 = 0.5$ ).

the elimination of three switches. But the limited-voltage and shoot-through problems still remain. In order to solve them, the DC-DC boost converter is replaced by a Z-network in [57], in which five switches are eliminated. However, there are still nine switches left in it.

To reduce the number of switches further, a dual-output Z-source half-bridge converter with only three switches is proposed for hybrid electric vehicle systems [78] along with the impedance-network matching and design methodology in this section.

#### 8.2.1. System design

As mentioned above, electric vehicles require power supplies with dual-output DC-AC converters, because there are two energy systems. Moreover, specific features such as few switches, being immune to the shoot-through problem, and high output-voltage gains are eagerly required. Therefore, the impedance-matching is used to analyse the disadvantages of traditional converters and to improve them. Then, the half-bridge DC-AC converter topology is chosen, because it contains only two switches.

Since it can reduce the output impedance, parallel connectivity is employed in realising output-impedance matching. Moreover, to provide two output voltages, two half-bridge DC-AC converters are placed in parallel. In order to use as few switches as possible and inspired by the nine-switches converter, one capacitor and one switch are shared by two converters, which results in the novel converter as shown in Fig. 22. Further, to provide immunity to the shoot-through problem and high output-voltage gains, an X-shaped two-port impedance-network is embedded into the traditional half-bridge converter in terms of Table 3, which finally results in the novel converter as shown in Fig. 23.

The proposed converter is depicted in Fig. 23, in which two outputs share the same capacitor  $C_{d2}$  and the same switch  $S_2$ . Thus, the proposed converter exhibits the same features as the Z-source half-bridge converter in Fig. 18. Therein, capacitors  $C_{d1}$ ,  $C_{d2}$ , and switches  $S_1$ ,  $S_2$  offer a loop for the load  $Gen$ , while capacitors  $C_{d2}$ ,  $C_{d3}$  and switches

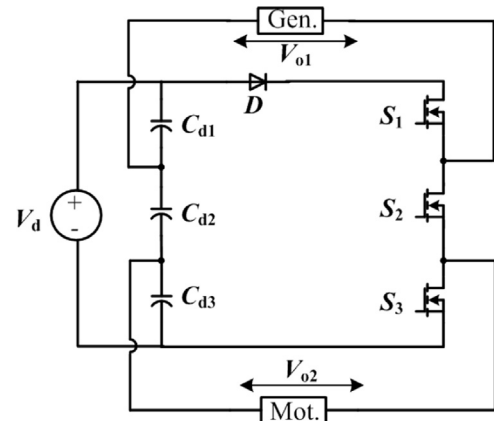


Fig. 22. A dual-output half-bridge converter with three switches.

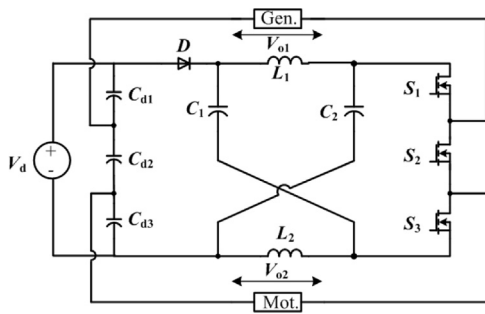


Fig. 23. A dual-output Z-source half-bridge converter with three switches.

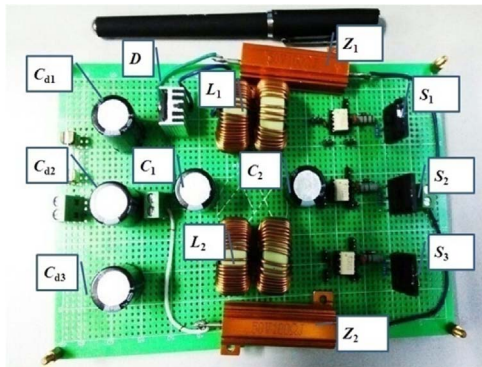


Fig. 24. Prototype of the proposed converter.

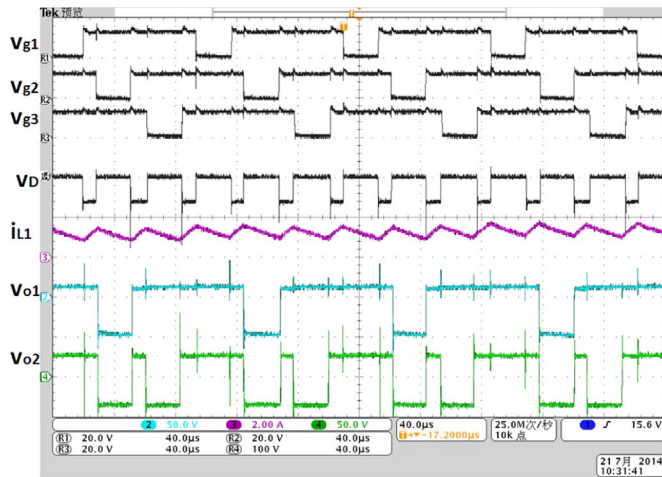


Fig. 25. Experimental waveforms in the shoot-through case.

$S_2, S_3$  form another loop for the load *Mot*, and these two loops share the same Z-network, consisting of capacitors  $C_1, C_2$  and inductors  $L_1, L_2$ . Due to the Z-network, the proposed converter solves the shoot-through and limited-voltage problems well. The unique feature of the proposed converter is that there are only three switches, which reduce its cost and increase the efficiency of electric vehicles.

### 8.2.2. Experimental verification

The prototype shown in Fig. 24 is composed of  $C_{d1}, C_{d2}, C_{d3}, L_1, L_2, C_1, C_2$ , diode  $D$  (of type MBRF20200), switches  $S_1, S_2, S_3$  (of type IRFP250A), and the resistive loads  $Z_1, Z_2$ , with the driving circuits located on the left side of each switch. The three circuits are driven by three generated synchronous driving signals coming from the RT-lab equipment (of type OP5600), and driving ICs TLP2.

Fig. 25 presents the experimental waveforms obtained for the converter operating with  $\Delta d = \frac{1}{3}$  and  $d_c = 0.75$ . Therein, the driven voltages of three switches  $v_{g1}, v_{g2}, v_{g3}$ , the diode voltage  $v_D$ , the current of

$L_1, i_{L1}$ , and the two output voltages  $v_{o1}, v_{o2}$  are depicted. In detail, the negative and positive output voltages of  $Z_1$  are asymmetric. The positive one is about 15 V, and the negative one is nearly equal to  $V_d/2$ , and the width is  $d_c T$ ; while the negative one is  $-45$  V, which is much larger than  $V_d/2$ . Moreover, the negative and positive output voltages of  $Z_2$  are symmetric in amplitude, namely  $\pm 30$  V, and their widths can be modulated. The experimental results are also consistent with the simulation results.

## 9. Conclusion

This paper has briefly expounded the development history of power electronics (converters) and reviewed various converters used in the past and currently. Then, a qualitative analysis has been conducted to explain the problems of conventional converters, like shoot-through, open-circuit, and limited output-voltage/current gain, which greatly hinder wide applications of power electronics in industry. This analysis reveals, in turn, that the newly proposed impedance-source converters can overcome these problems, demonstrating great potential for industrial applications, especially in renewable energy systems.

A further analysis derives a set of criteria for designing impedance-source converters, which leads to a design methodology dealing with input- and output-impedance matching, and with load-phase matching. This overcomes the shortcomings of the traditional tedious, manual and experience-dependent design methods and eases the design of new converters. With this design methodology, a Z-source half-bridge converter for electroplating applications and a dual-output Z-source half-bridge converter for hybrid electric vehicles have been designed.

It is expected that a variety of impedance-source converters will to be designed in the near future addressing the needs of specific industrial applications.

## Acknowledgement

This work was supported by the National Natural Science Foundation of China (Grant Nos. U1501251 and 51307025), the Foundation for Distinguished Young Talents in Higher Education of Guangdong (Grant No. 2016KQNCX039), the central financial support from the local colleges and universities development special fund project (Department of Financial and Education of Guangdong Province 2016 [202]) and the Research Group Linkage grant No. 2.4-IP-DEU/1009882 by the Alexander von Humboldt Foundation.

## References

- [1] Moller P, Kramer B. Review: electric fish. *Biosci (Am Inst Biol Sci)* 1991;44(11):794–800.
- [2] Stewart J. Intermediate electromagnetic theory. *BioScience (World Scientific)*. ISBN 981-02-4471-1; 2001. p. 50.
- [3] Simpson B. Electrical stimulation and the relief of pain. *Elsevier Health Sci* 2003;6–7, [ISBN 0-444-51258-6].
- [4] Chenari B, Carrilho JD, da Silva MG. Towards sustainable, energy-efficient and healthy ventilation strategies in buildings: a review. *Renew Sustain Energy Rev* 2016;59:1426–47.
- [5] Moradi MH, Razini S, Hosseini SM. State of art of multiagent systems in power engineering: a review. *Renew Sustain Energy Rev* 2016;58:814–24.
- [6] Keithley JF. The story of electrical and magnetic measurements: from 500 BC to the 1940s. Piscataway, NJ: Wiley-IEEE Press; 1999. p. 20, [ISBN 0-7803-1193-0].
- [7] Masters GM. Renewable and efficient electric power systems. Hoboken, New Jersey: John Wiley & Sons; 2013.
- [8] Abdel-Salam M. High-voltage engineering: theory and practice, revised and expanded. New York: CRC Press; 2000.
- [9] Jeszenszky S. History of transformers. *IEEE Power Eng Rev* 1996;16(12):9.
- [10] Kouhnavard M, Ikeda S, Ludin NA, Khairudin NA, Ghaffari BV, Mat-Teridi MA, et al. A review of semiconductor materials as sensitizers for quantum dot-sensitized solar cells. *Renew Sustain Energy Rev* 2014;37:397–407.
- [11] Zhang B, Qiu D. Sneak circuits of power electronic converters. Singapore: John Wiley & Sons; 2014.
- [12] Justo JJ, Mwasilu F, Lee J, Jung JW. AC-microgrids versus DC-microgrids with distributed energy resources: a review. *Renew Sustain Energy Rev*

- 2013;24:387–405.
- [13] Planas E, Gil-de-Muro A, Andreu J, Kortabarria I, de Alegria IM. General aspects, hierarchical controls and droop methods in microgrids: a review. *Renew Sustain Energy Rev* 2013;17:147–59.
- [14] Mwasilu F, Justo JJ, Kim EK, Do TD, Jung JW. Electric vehicles and smart grid interaction: a review on vehicle to grid and renewable energy sources integration. *Renew Sustain Energy Rev* 2014;34:501–16.
- [15] Van Hertem D, Ghandhari M. Multi-terminal VSC HVDC for the European supergrid: obstacles. *Renew Sustain Energy Rev* 2010;14(9):3156–63.
- [16] Akorede MF, Hizam H, Poursamael E. Distributed energy resources and benefits to the environment. *Renew Sustain Energy Rev* 2010;14(2):724–34.
- [17] Ming T, Wu Y, Liu W, Sherif SA. Solar updraft power plant system: a brief review and a case study on a new system with radial partition walls in its collector. *Renew Sustain Energy Rev* 2017;69:472–87.
- [18] Bose BK. *Power electronics and motor drives: advances and trends*. Burlinto, USA: Academic Press; 2010.
- [19] Steimer PK, Gruning HE, Werninger J, Carroll E, Klaka S, Linder S. IGBT-a new emerging technology for high-power, low-cost inverters. *IEEE Ind Appl Mag* 1999;5(4):12–8.
- [20] Colak I, Kabalci E, Bayindir R. Review of multilevel voltage source inverter topologies and control schemes. *Energy Convers Manag* 2011;52(2):1114–28.
- [21] Peng FZ. Z-source inverter. *IEEE Trans Ind Appl* 2003;39(2):504–10.
- [22] Siwakoti Y, Peng F, Blaabjerg F. Impedance-source networks for electric power conversion part I: a topological review. *IEEE Trans Power Electron* 2015;30(2):699–716.
- [23] Siwakoti Y, Peng F, Blaabjerg F. Impedance-source networks for electric power conversion part II: review of control and modulation techniques. *IEEE Trans Power Electron* 2015;30(4):1887–906.
- [24] Ellabban O, Abu-Rub H. An overview for the Z-source converter in motor drive applications. *Renew Sustain Energy Rev* 2016;61:537–55.
- [25] Suganthi J, Rajaram M. Effective analysis and comparison of impedance source inverter topologies with different control strategies for power conditioning system. *Renew Sustain Energy Rev* 2015;51:821–9.
- [26] Kirubakaran A, Jain S, Nema RK. A review on fuel cell technologies and power electronic interface. *Renew Sustain Energy Rev* 2009;13(9):2430–40.
- [27] Ellabban O, Abu-Rub H. Z-source inverter: topology improvements review. *IEEE Ind Electron Mag* 2016;10(1):6–24.
- [28] Zhang G, Zhang B, Li Z, Qiu D, Yang L, Halang WA. A 3-Z-network boost converter. *IEEE Trans Ind Electron* 2015;62(1):278–88.
- [29] Zhang G, Lu HH, Zhang B, Li Z, Fernando T, Chen S-Z, Zhang Y. An impedance networks boost converter with high-voltage gain, to appear in *IEEE Trans Power Electron*.
- [30] Sun D, Ge B, Yan X, Bi D, Zhang H, Liu Y, et al. Modeling, impedance design, and efficiency analysis of quasi-Z-source module in cascaded multilevel photovoltaic power system. *IEEE Trans Ind Electron* 2014;61(11):6108–17.
- [31] Franke WT, Mohr M, Fuchs FW. Comparison of a Z-source inverter and a voltage-source inverter linked with a dc/dc-boost-converter for wind turbines concerning their efficiency and installed semiconductor power. In: *Proceedings of the IEEE power electronics specialists conference*; 2008. p. 1814–20.
- [32] Tran QV, Chun TW, Ahn JR, Lee HH. Algorithms for controlling both the DC boost and AC output voltage of Z-source inverter. *IEEE Trans Ind Electron* 2007;54(5):2745–50.
- [33] Ge B, Abu-Rub H, Peng FZ, Lei Q, de Almeida AT, Ferreira FJ, et al. An energy-stored quasi-Z-source inverter for application to photovoltaic power system. *IEEE Trans Ind Electron* 2013;60(10):4468–81.
- [34] Choi WY, Lee CG. Photovoltaic panel integrated power conditioning system using a high efficiency step-up DC-DC converter. *Renew Energy* 2012;41:227–34.
- [35] Peng FZ, Yuan X, Fang X, Qian Z. Z-source inverter for adjustable speed drives. *IEEE Trans Power Electron Lett* 2003;1(2):33–5.
- [36] Dehghan SM, Mohamadian M, Yazdian A, Ashrafzadeh F. A dual-input-dual-output Z-source inverter. *IEEE Trans Power Electron* 2010;25(2):360–8.
- [37] Dehghan SM, Mohamadian M, Yazdian A. Hybrid electric vehicle based on bidirectional Z-source nine-switch inverter. *IEEE Trans Veh Technol* 2010;59(6):2641–53.
- [38] Ge BM, Lei Q, Qian W, Peng FZ. A family of Z-source matrix converters. *IEEE Trans Ind Electron* 2012;59(1):35–46.
- [39] Ismail EH, Al-Saffar MA, Sabzali AJ, Fardoun AA. A family of single-switch PWM converters with high step-up conversion ratio. *IEEE Trans Circ Syst I* 2008;55(4):1159–71.
- [40] Wikipedia. *Electrical Impedance*, ([http://www.en.wikipedia.org/wiki/Electrical\\_impedance](http://www.en.wikipedia.org/wiki/Electrical_impedance)).
- [41] Neill TBM. Generalisation of nodal and mesh analysis. *Electron Lett* 1969;5(16):365–6.
- [42] Haykin SS. *Active network theory*. Addison-Wesley; 1970.
- [43] Egan WF. *Practical RF system design*. Hoboken, New Jersey: Wiley-IEEE; 2003.
- [44] Jaeger RC, Blalock TN. *Microelectronic circuit design*, 3rd ed.. McGraw-Hill Press; 2006.
- [45] Ghosh S. *Network theory: analysis and synthesis*. India: Prentice Hall of India; 2005.
- [46] Wikipedia. *Two-port network*, ([http://en.wikipedia.org/wiki/Two-port\\_network](http://en.wikipedia.org/wiki/Two-port_network)).
- [47] Chen L, Peng FZ. Dead-time elimination for voltage source inverters. *IEEE Trans Power Electron* 2008;23(2):574–80.
- [48] Sun PW. *Cascade dual-buck inverters for renewable energy and distributed generation* (Ph.D. diss.). Virginia, USA: Virginia Polytechnic Institute and State University; 2012.
- [49] Peng FZ, Shen M, Qian Z. Maximum boost control of the Z-source inverter. *IEEE Trans Power Electron* 2005;20(4):833–8.
- [50] Loh PC, Vilathgamuwa DM, Lai YS, Chua GT, Li Y. Pulse-width modulation of Z-source inverters. In: *Proceedings of the conference record of the 2004 IEEE industry applications conference, 39th IAS annual meeting*; 1; 2004.
- [51] Gajanayake CJ, Vilathgamuwa DM, Loh PC. Development of a comprehensive model and a multiloop controller for Z-source inverter DG systems. *IEEE Trans Ind Electron* 2007;54(4):2352–9.
- [52] Loh PC, Vilathgamuwa DM, Gajanayake CJ, Wong LT, Ang CP. Z-source current-type inverters: digital modulation and logic implementation. In: *Proceedings of the conference record of the 2005 industry applications conference, Fourtieth IAS annual meeting*; 2005. p. 940–7.
- [53] Gajanayake CJ, Vilathgamuwa DM, Loh PC, Teodorescu R, Blaabjerg F. Z-source inverter-based flexible distributed generation system solution for grid power quality improvement. *IEEE Trans Energy Convers* 2009;24(3):695–704.
- [54] Tang Y, Xie S, Zhang C. An improved-source inverter. *IEEE Trans Power Electron* 2011;26(12):3865–8.
- [55] Tang Y, Xie S, Zhang C. Single-phase Z-source inverter. *IEEE Trans Power Electron* 2011;26(12):3869–73.
- [56] Jung JW, Keyhani A. Control of a fuel cell based Z-source converter. *IEEE Trans Energy Convers* 2007;22(2):467–76.
- [57] Dehghan SM, Mohamadian M, Yazdian Varjani A. Hybrid electric vehicle based on bidirectional Z-source nine-switch inverter. *IEEE Trans Veh Technol* 2010;59(6):2641–53.
- [58] Vinnikov D, Roasto I, Strzelecki R, Adamowicz M. Step-up DC-DC converters with cascaded quasi-Z-source network. *IEEE Trans Ind Electron* 2012;59(10):3727–36.
- [59] Anderson J, Peng FZ. Four quasi-Z-source inverters. In: *Proceedings of the IEEE power electronics specialists conference (PESC 2008)*; 58(1); 2008. p. 2743–9.
- [60] Cao D, Peng FZ. A family of Z-source and quasi-Z-source DC-DC converters. In: *Proceedings of the Twenty-Fourth Annual IEEE applied power electronics conference and exposition (APEC 2009)*; 58(1); 2009. p. 1097–101.
- [61] Vinnikov D, Roasto I. Quasi-Z-source-based isolated DC-DC converters for distributed power generation. *IEEE Trans Ind Electron* 2011;58(1):192–201.
- [62] Qian W, Peng FZ, Cha H. Trans-Z-source inverters. *IEEE Trans Power Electron* 2011;26(12):3453–63.
- [63] Loh PC, Gao F, Blaabjerg F. Embedded EZ-source inverters. *IEEE Trans Ind Appl* 2010;46(1):256–67.
- [64] Siwakoti Y, Loh PC, Blaabjerg F, Town G. Y-source impedance network. *IEEE Trans Power Electron* 2014;29(7):3250–4.
- [65] Loh PC, Li D, Blaabjerg F. *F-Z-source inverters*. *IEEE Trans Power Electron Lett* 2013;28(11):4880–4.
- [66] Mo W, Loh PC, Blaabjerg F. Asymmetrical *F*-source inverters. *IEEE Trans Ind Electron* 2014;61(2):637–47.
- [67] Mo W, Loh PC, Blaabjerg F. Voltage type *F*-source inverters with continuous input current and enhanced voltage boost capability. In: *Proceedings of the 15th International power electronics and motion control conference and exposition Europe congress*; 2012.
- [68] Loh PC, Li D, Blaabjerg F. Current-type flipped-*F*-source inverters. In: *Proceedings of the 7th International power electronics and motion control conference (IPEMC)*; 1; 2012. p. 594–8.
- [69] Adamowicz M. LCCT-Z-source inverters. In: *Proceedings of the 10th International conference on environment and electrical engineering (EEEIC)*; 2011. p. 1–6.
- [70] Adamowicz M, Strzelecki R, Peng FZ, Guzinski J, Rub HA. New type LCCT-Z-source inverters. In: *Proceedings of the 14th European conference on power electronics and applications (EPE 2011)*; 2011. p. 1–10.
- [71] Zhang F, Peng FZ, Qian Z. Z-H converter. In: *Proceedings of the IEEE power electronics specialists conference (PESC 2008)*; 2008. p. 1004–7.
- [72] Hu X, Ling ZY, He XH, Chen SS. Controlling transmission spectra of photonic crystals under electrochemical oxidization of aluminum. *J Electrochem Soc* 2009;156(5):C176–C179.
- [73] Hu X, Ling ZY, Sun TL, He XH. Tuning optical properties of photonic crystal of anodic alumina and the influence of electrodeposition. *J Electrochem Soc* 2009;156(11):D521–D524.
- [74] Stout PJ, Zhang D. High-power magnetron Cu seed deposition on 3-D dual inlaid features. *IEEE Trans Plasma Sci* 2002;30(1):116–7.
- [75] Zhang WM, Deng MH, Pei YQ, Wang ZA. Design and optimization of high current power supply for electrochemistry. In: *Proceedings of the IPEC*; 2010. p. 86–91.
- [76] Zhang G, Li Z, Zhang B, Qiu D, Xiao W, Halang WA. A Z-source half-bridge converter. *IEEE Trans Ind Electron* 2014;61(3):1269–79.
- [77] Liu J, Peng H. Modeling and control of a power-split hybrid vehicle. *IEEE Trans Control Syst Technol* 2008;16(6):1242–51.
- [78] Zhang G, Zhang B, Li Z, Zhang Y, Chen S-Z. A novel single-input-dual-output impedance network converter, to appear in *IEEE J Emerg Sel Top Power Electron*.